

RESEARCH ARTICLE

10.1002/2013JD020715

Key Points:

- First measurements of nitrate isotopic composition from a tropical ice core
- Postdepositional alteration appears limited throughout most of the record
- Seasonal changes may reflect NO_x sources and atmospheric oxidation chemistry

Supporting Information:

- Readme
- Figure S1
- Figure S2
- Figure S3

Correspondence to:

A. M. Buffen,
aron_buffen@brown.edu

Citation:

Buffen, A. M., M. G. Hastings, L. G. Thompson, and E. Mosley-Thompson (2014), Investigating the preservation of nitrate isotopic composition in a tropical ice core from the Quelccaya Ice Cap, Peru, *J. Geophys. Res. Atmos.*, *119*, 2674–2697, doi:10.1002/2013JD020715.

Received 19 AUG 2013

Accepted 24 JAN 2014

Accepted article online 30 JAN 2014

Published online 13 MAR 2014

Investigating the preservation of nitrate isotopic composition in a tropical ice core from the Quelccaya Ice Cap, Peru

Aron M. Buffen¹, Meredith G. Hastings¹, Lonnie G. Thompson², and Ellen Mosley-Thompson³

¹Department of Geological Sciences and Environmental Change Initiative, Brown University, Providence, Rhode Island, USA,

²School of Earth Sciences and Byrd Polar Research Center, Ohio State University, Columbus, Ohio, USA, ³Department of Geography and Byrd Polar Research Center, Ohio State University, Columbus, Ohio, USA

Abstract The nitrogen and oxygen isotopic composition of nitrate in ice cores offers unique potential for examining reactive nitrogen oxide (NO_x) budgets and oxidation chemistry of past atmospheres. A low-latitude record is of particular interest given that the dominant natural sources of NO_x and production of hydroxyl radical are most prevalent in the tropics. Any interpretation of nitrate in ice cores, however, must first consider that nitrate in snow is vulnerable to postdepositional loss and isotopic alteration. We report and assess the integrity of nitrate- $\delta^{15}\text{N}$, $-\delta^{18}\text{O}$, and $-\Delta^{17}\text{O}$ in a 30 m ice core from a high-elevation site in the central Andes. Clear seasonality in $\delta^{15}\text{N}$, $\delta^{18}\text{O}$, and nitrate concentration exists throughout most of the record and cannot be explained by photolysis or evaporation based on our current understanding of these processes. In contrast, nitrate in the upper ~12 m of the core and in a snowpit shows very different behavior. This may reflect alteration facilitated by recent melting at the surface. The relationships between $\delta^{15}\text{N}$, $\delta^{18}\text{O}$, $\Delta^{17}\text{O}$, and concentration in the unaltered sections can be interpreted in terms of mixing of nitrate from discrete sources. Transport effects and an englacial contribution from nitrification cannot be ruled out at this time, but the observed isotopic compositions are consistent with expected signatures of known NO_x sources and atmospheric oxidation pathways. Specifically, nitrate deposited during the wet season reflects biogenic soil emissions and hydroxyl/peroxy radical chemistry in the Amazon, while dry season deposition reflects a lightning source and ozone chemistry at higher levels in the troposphere.

1. Introduction

Reactive nitrogen oxides (NO_x = NO + NO₂) are of fundamental importance to the chemistry of the troposphere. The formation and fate of NO_x has implications for air quality, ecosystem health, and the composition of the atmosphere. Photochemical cycling of NO_x in the presence of volatile organic compounds, methane, and carbon monoxide produces ozone (O₃), a major air pollutant and potent greenhouse gas in the troposphere [Anenberg *et al.*, 2009]. Oxidation of NO_x by O₃ or the hydroxyl radical (OH) forms nitrate (NO₃⁻), an important and often limiting micronutrient [Elser *et al.*, 2009; Holtgrieve *et al.*, 2011] and a primary component of acid rain in the form of nitric acid (HNO₃) [Likens and Bormann, 1974]. Together, concentrations of OH and O₃ determine the oxidizing capacity of the atmosphere and regulate the lifetimes of trace gases such as methane [Thompson, 1992]. NO_x emission and nitrate deposition can also affect planetary radiative balance via direct and indirect aerosol effects and the potential to alter ecosystem carbon storage [Shindell *et al.*, 2009; Janssens *et al.*, 2010].

Over the past 150 years, NO_x emissions have increased globally as a result of fossil fuel and biofuel combustion, biomass burning, and aircraft emissions [Galloway *et al.*, 2004]. Important natural inputs of NO_x to the troposphere include biomass burning, soil microbial emissions, and lightning, with minor contribution from stratospheric injection and ammonia oxidation [Delmas *et al.*, 1997; Lee *et al.*, 1997]. Past variability in NO_x mixing ratios and the relative contribution of these sources, however, remain poorly constrained, and effects on the oxidizing capacity of the atmosphere through time are unclear.

The utility of atmospheric nitrate as a paleoenvironmental proxy (e.g., biomass burning and lightning) and in reconstructing NO_x concentrations has long motivated its study in ice cores. Nitrate concentrations ([NO₃⁻]) in snow have been shown to reflect changes in atmospheric loading [Mayewski *et al.*, 1990; Schwikowski *et al.*, 1999], but quantitative assessments of atmospheric mixing ratios based on [NO₃⁻] have been hindered by a

susceptibility to postdepositional loss, while the partitioning of NO_x inputs is complicated by the fact that concentration alone is not diagnostic of individual sources.

Measurement of nitrogen and oxygen stable isotope ratios in nitrate provides a complementary approach to reconstructing precursor NO_x dynamics through time. Oxygen isotope ratios reflect relative abundances of oxidants and the reaction pathways by which they convert NO_x to nitrate (section 5.6.1) [Michalski *et al.*, 2003, 2011; Alexander *et al.*, 2004, 2009; Kendall *et al.*, 2007; Jarvis *et al.*, 2008, 2009; Kunasek *et al.*, 2008]. The nitrogen isotopic composition, on the other hand, can contain a signature imprinted by the respective NO_x source (section 5.6.2) [e.g., Hoering, 1957; Heaton, 1986; Hastings *et al.*, 2003, 2009; Elliott *et al.*, 2007, 2009; Kendall *et al.*, 2007; Savarino *et al.*, 2007; Li and Wang, 2008; Felix *et al.*, 2012].

Most of these studies have taken place in the mid and high latitudes, and work focusing on archives contained in snow and ice have been confined, unsurprisingly, to polar regions (see Savarino and Morin [2011] for a summary), the European Alps [Freyer *et al.*, 1996; Pichlmayer *et al.*, 1998], and the Rocky Mountains [Naftz *et al.*, 2011]. Isotopic studies of atmospheric nitrate in the tropics (23.4°N-S) have been sparse and, to our knowledge, limited to Ecuadorian rain, stream and fog water [Brothers *et al.*, 2008; Fabian *et al.*, 2009; Schwarz *et al.*, 2011], aerosols and rain over the Atlantic Ocean [Baker *et al.*, 2007; Alexander *et al.*, 2009; Morin *et al.*, 2009], and salt deposits in the Atacama Desert of Chile [Michalski *et al.*, 2004a, and references therein].

The dominant natural sources of NO_x , however, are located in the tropics as is production of OH [Yienger and Levy, 1995; Lee *et al.*, 1997; Crutzen and Lelieveld, 2001; Jaeglé *et al.*, 2005]. Given the short residence times of NO_x (hours to days) and nitrate (days as HNO_3 ; up to weeks as organic nitrate) in the lower troposphere relative to the interhemispheric mixing time (~ 1 year), concentrations of these species are highly heterogeneous in the atmosphere. As such, the spatial context within which a given record of atmospheric nitrate can be interpreted will be largely regional.

Tropical ice core records of nitrate isotopic composition thus hold a unique potential for reconstructing NO_x and oxidant variability in key source regions and add to the suite of paleoenvironmental proxies available from these archives (e.g., as a biomass burning indicator). Such reconstructions would provide useful validation for models [Levy *et al.*, 1999; Alexander *et al.*, 2009] and can bridge higher-latitude studies in establishing a more global perspective. A serious potential caveat, however, is that nitrate can be lost from the snowpack by processes which are isotopically fractionating, and where significant, this will preclude an accurate interpretation of the record ultimately preserved in the ice below. As such, any study of nitrate in ice cores must first assess the extent to which such postdepositional processing has occurred.

The work presented here takes this approach in developing the first tropical ice core record of nitrate isotopic composition. Using a 30 m core drilled from the Quelccaya Ice Cap, southeastern Peru, that spans the period ~ 1980 to 2003, we find that the effects of photolysis and evaporation of HNO_3 have been limited or negligible throughout much of the record. In contrast, the more recent portion of the core (~ 1997 to 2003) and a 2 m snowpit sampled in 2011 appear to have been isotopically altered. The fractionating processes by which this has occurred are difficult to distinguish but may have been facilitated by meltwater leaching of nitrate induced by recent warming at the site. We conclude that interpreting the isotopic composition of the unaltered portions of the core in terms of source and oxidant signatures should be possible and that this potential also exists for other tropical glaciers where conditions are suitable.

2. Site Description

The Quelccaya Ice Cap (QIC) is the largest tropical ice cap on Earth (Figures 1 and S1; 13.93°S , 70.83°W ; $\sim 55 \text{ km}^2$) [Thompson *et al.*, 1985]. It is located in the Cordillera Vilcanota along the northeastern boundary of the Altiplano, a broad, high-elevation plateau that defines the topography of the central Andes between ~ 13 and 22°S (~ 4000 m above sea level (asl) mean elevation).

Precipitation over the Altiplano is highly seasonal with 50 to 80% of the annual total falling between December and February in alternating, \sim weeklong wet/dry episodes [Vuille *et al.*, 2000]. During the wet season (December–February), deep convection is fueled by low-level moisture from the Amazon Basin that is promoted upslope and onto the plateau by strong, upper level easterly winds [Garreaud *et al.*, 2003]. During the dry season (June–August), this low-level flux from the Amazon is suppressed by westerly flow

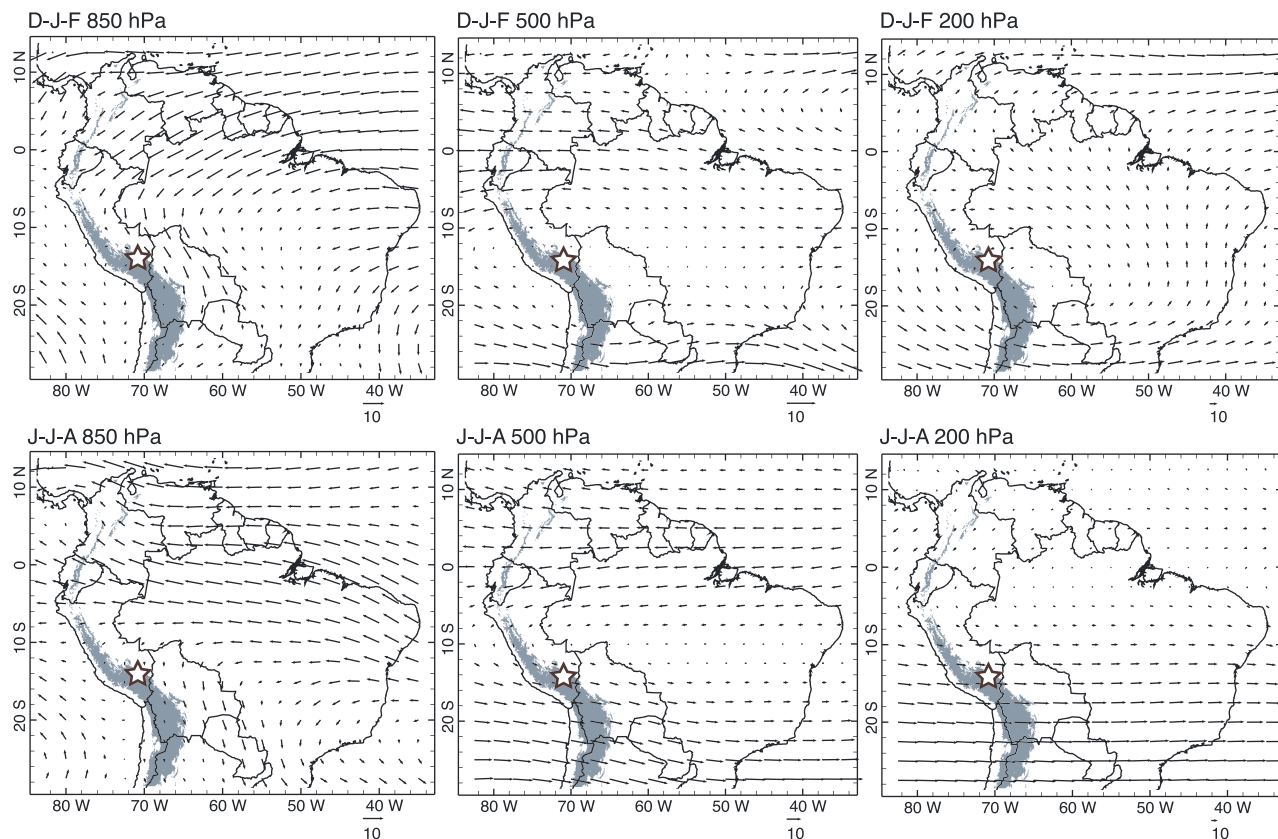


Figure 1. Location of the Quelccaya Ice Cap (open star) and regional atmospheric circulation patterns at the 850, 500, and 200 hPa levels for December–January–February (wet season) and June–July–August (dry season) averaged over the period 1980–2009 (NCEP–DOE Reanalysis-2 [Kanamitsu *et al.*, 2002]). Geopotential heights of the three pressure levels are roughly 1.5, 5.9, and 12.4 km over the central Andes, respectively. Note that the scale arrows for wind speed, in units of m s^{-1} , differ in size. Shaded areas represent elevations above 3000 m asl.

aloft, while the contribution of moist air from the eastern Pacific is inhibited by sharp coastal topography, large-scale subsidence, and a strong temperature inversion over the cool surface waters.

Net accumulation at the QIC summit (5670 m asl) is ~ 2 to 3 m snow yr^{-1} , and mean annual air temperature is -4.3°C based on automated weather station measurements from June 2007 through July 2012 (D. Hardy, personal communication, 2013). Average daily temperatures during December–March and June–September are -5.0 and -3.6°C , though daily maxima during the wet season often exceeded the freezing point [Bradley *et al.*, 2009; D. Hardy, personal communication, 2013].

3. Methods

3.1. Sample Collection

In August 2003, a 29.97 m ice core (QND30) was recovered from the northern dome (5620 m asl) of the QIC by members of the Byrd Polar Research Center (BPRC) of The Ohio State University as part of a larger drilling initiative on the ice cap (Figure S1). The firn-ice transition at the drill site was located below $\sim 23 \text{ m}$ based on density measurements. The unconsolidated top 0.18 m of the core was lost during the drilling. QND30 was drilled electromechanically without the use of fluid.

The core was returned frozen to the BPRC and stored at -30°C prior to sampling in 2010. All samples were cut by bandsaw in a -10°C facility at $\sim 10 \text{ cm}$ resolution, and $\sim 1 \text{ cm}$ of each outer surface was discarded. Individual samples, excluding those from sections of snow and firn, were then rinsed with ultrapure Millipore Milli-Q water and melted at room temperature in precleaned, high-density polyethylene bottles (HDPE) prior to analysis.

Table 1. Pooled Standard Deviations^a ($1\sigma_p$) in ‰ and Total Sample Size (n) of Standards Run Within Sample Sets and Sample Replicates Run in Separate Sets^b

$1\sigma_p$ (n)	IAEA-NO-3	USGS-34	USGS-35	Sample Replicates
$\delta^{15}\text{N}$	0.3 (92)	0.2 (92)	-	0.5 (108)
$\delta^{18}\text{O}$	0.5 (92)	0.5 (92)	0.6 (93)	0.8 (108)
$\Delta^{17}\text{O}$	-	0.4 (39)	0.5 (39)	0.6 (7)
Standard Values	IAEA-NO-3	USGS-34	USGS-35	Reference
$\delta^{15}\text{N}$	4.7	-1.8	-	<i>Böhlke et al. [2003]</i>
$\delta^{18}\text{O}$	25.6	-27.9	57.5	<i>Böhlke et al. [2003]</i>
$\Delta^{17}\text{O}^c$	-	-0.3	21.6	<i>Michalski et al. [2002]</i>

^a $\sigma_p = \sqrt{\frac{\sum_{i=1}^k (n_i - 1) s_i^2}{\sum_{i=1}^k (n_i - 1)}}$, where n_i and s_i^2 are the size and variance of the i th set of samples, respectively, and k is the total number of sets.

^bAlso listed are the accepted reference values for $\delta^{15}\text{N}$ versus $\text{N}_{2\text{-air}}$ and for $\delta^{18}\text{O}$ and $\Delta^{17}\text{O}$ versus VSMOW for the calibration standards used. Within a run, samples and standards are analyzed at similar concentrations and in equivalent amounts (10–5 nmol for $\delta^{15}\text{N}$ and $\delta^{18}\text{O}$; 50–35 nmol for $\Delta^{17}\text{O}$).

^cCalculated using the linear definition $\Delta^{17}\text{O} = \delta^{17}\text{O} - 0.52 \cdot \delta^{18}\text{O}$.

In July 2011, a 2.10 m snowpit was sampled at the QIC summit dome (5670 m asl) at 2 to 10 cm intervals (Figure S1). These samples were melted in the field in precleaned HDPE bottles sealed with Parafilm and returned as liquid to Brown University where they were stored at -20°C . The samples were not exposed to sunlight and were kept as liquid for less than 3 days.

3.2. Laboratory Analysis

Nitrate and nitrite (NO_2^-) concentrations were measured photometrically using a Westco Scientific SmartChem 200 discrete chemistry analyzer. The pooled standard deviation ($1\sigma_p$) of $[\text{NO}_3^-]$ in 85 control standards run within sets of samples was $0.10 \mu\text{mol L}^{-1}$ (μM ; 6.2 ppb NO_3^-). Nitrite, which is not discriminated from nitrate in the isotopic analyses described below, was consistently at or below detection limits as determined by system blanks ($[\text{NO}_3^-] = 0.09 \mu\text{M}$ and $[\text{NO}_2^-] = 0.05 \mu\text{M}$).

Isotopic composition was analyzed following the denitrifier method developed by *Sigman et al. [2001]* and *Casciotti et al. [2002]*. This method utilizes denitrifying bacteria to convert NO_3^- to nitrous oxide ($\text{N}_2\text{O}_{(\text{g})}$) which is then captured and injected into an isotope ratio mass spectrometer (IRMS) in continuous flow mode. At Brown, the technique requires as little as 5 nmol nitrate-N and is thus suited to the low-concentration, low-volume samples typical of ice core research.

Isotope ratios are reported using delta notation ($\delta^{15}\text{N}$ and $\delta^{18}\text{O}$),

$$\delta = \left(\frac{R_{\text{sample}}}{R_{\text{reference}}} - 1 \right) \cdot 10^3 \text{ ‰}, \quad (1)$$

where $R = {}^{15}\text{N}/{}^{14}\text{N}$ or ${}^{18}\text{O}/{}^{16}\text{O}$, and values are referenced to atmospheric N_2 and Vienna Standard Mean Ocean Water (VSMOW), respectively, in units of per mil (‰). All isotope measurements were made using a Thermo Scientific Delta V Plus IRMS, and the data were calibrated using the IAEA-NO-3, USGS-34, and USGS-35 nitrate reference standards (Table 1).

We report precision in two ways: the $1\sigma_p$ of all standards run within sample sets and the $1\sigma_p$ of replicate samples run in at least two different sets (Table 1). These measures account for variance derived from both sample preparation and isotopic analysis and thus represent the overall method precision rather than instrumental precision.

The bacterial strain used (*Pseudomonas aureofaciens*) promotes a limited exchange of oxygen between water and the intermediates of denitrification. This amounts to less than 10%, and frequently less than 3%, of the oxygen in the produced N_2O , and thus the $\delta^{18}\text{O}$ of nitrate is corrected using the measured $\delta^{18}\text{O}$ of water ($\delta^{18}\text{O}_{\text{water}}$) in the sample or standard (see *Casciotti et al. [2002]* and *Kaiser et al. [2007]* for further details). Sample $\delta^{18}\text{O}_{\text{water}}$ was measured at the BPRC using a Finnigan MAT Delta S Plus IRMS ($1\sigma = 0.2\text{‰}$). For 7% exchange, a difference greater than $\pm 10\text{‰}$ from the “true” $\delta^{18}\text{O}_{\text{water}}$ is required to affect the accuracy of our nitrate- $\delta^{18}\text{O}$ results by more than the method precision.

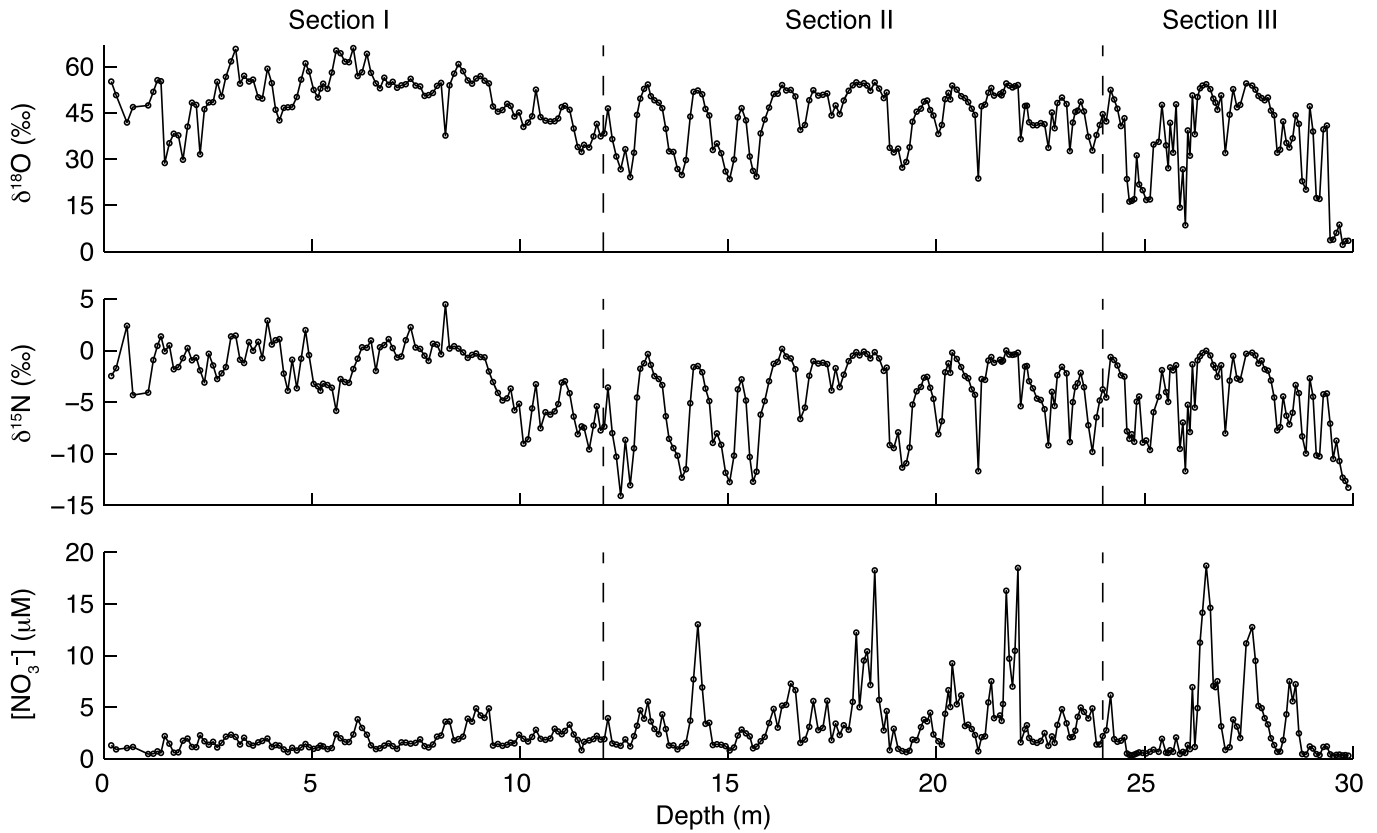


Figure 2. QND30 $\delta^{18}\text{O}$, $\delta^{15}\text{N}$, and $[\text{NO}_3^-]$ plotted by depth. Vertical dashed lines note the separation between Sections I (0–12 m), II (12–24 m), and III (24–30 m).

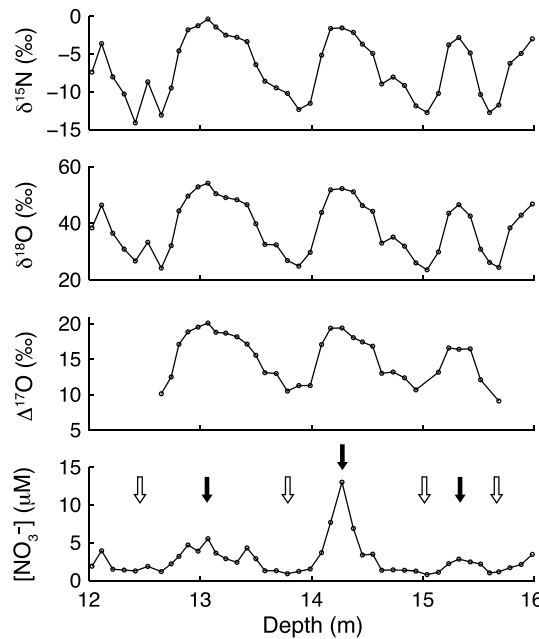


Figure 3. QND30 seasonality in $\delta^{15}\text{N}$, $\delta^{18}\text{O}$, $\Delta^{17}\text{O}$, and $[\text{NO}_3^-]$ highlighted between 12 and 16 m depth. Dry seasons (filled arrows) are marked by increased $[\text{NO}_3^-]$ and relatively enriched isotopic composition, while the opposite is true during wet seasons (open arrows). One seasonal cycle is represented by one $[\text{NO}_3^-]$ peak to the next.

The determination of $\delta^{15}\text{N}$ must account for isobaric interference of the $^{14}\text{N}^{14}\text{N}^{17}\text{O}$ isotopologue with $^{14}\text{N}^{15}\text{N}^{16}\text{O}$ at the m/z 45 signal measured by the IRMS [Kaiser et al., 2007]. For nitrate with an oxygen isotopic composition set by mass-dependent fractionation processes, this contribution can be removed by assuming $\delta^{17}\text{O} = 0.52 \cdot \delta^{18}\text{O}$ [Thiemens, 1999], where $\delta^{17}\text{O}$ corresponds to $R = ^{17}\text{O}/^{16}\text{O}$ in equation (1). This assumption is not necessarily valid, however, for atmospheric nitrate derived from the oxidation of NO_x by O_3 as the latter carries an anomalously high $\delta^{17}\text{O}$ signature (section 5.6.1) [Gao and Marcus, 2001; Savarino et al., 2008]. This “excess” of the ^{17}O isotope is referred to as $\Delta^{17}\text{O}$, where

$$\Delta^{17}\text{O} = \delta^{17}\text{O} - 0.52 \cdot \delta^{18}\text{O}, \quad (2)$$

and values are again expressed in ‰ versus VSMOW. A nonlinear definition also exists [Miller, 2002; Böhlke et al., 2003; Kaiser et al., 2007], but we use the linear form to remain consistent with previous work [e.g., Michalski et al., 2002, 2003, 2004a, 2004b, 2005; Alexander et al., 2004, 2009; McCabe et al., 2005; Morin et al., 2007a, 2007b, 2008, 2009, 2012; Patris et al., 2007; Savarino et al.,

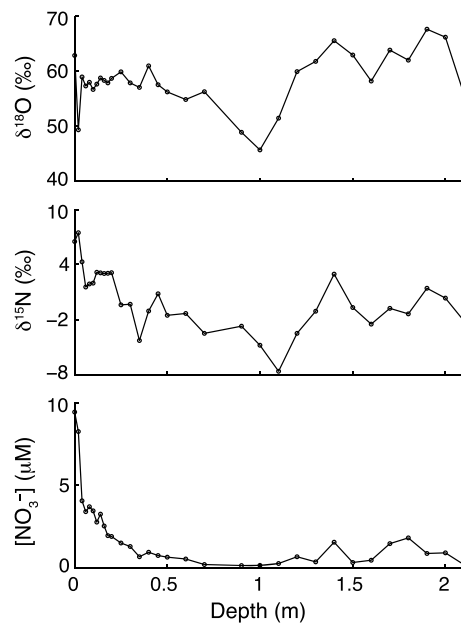


Figure 4. Snowpit $\delta^{18}\text{O}$, $\delta^{15}\text{N}$, and $[\text{NO}_3^-]$ plotted by depth.

2007; Kunasek et al., 2008; Frey et al., 2009; Erbland et al., 2013).

Underestimating this contribution will lead to an overestimate of $\delta^{15}\text{N}$ by as much as 1 to 2‰. We thus correct the QND30 data by using $\Delta^{17}\text{O}$ measured on a subset of 66 samples following the denitrifier approach of Kaiser et al. [2007] and referenced to the USGS-34 and USGS-35 standards (Table 1). This method involves thermally decomposing the N_2O product to O_2 for isotopic analysis and requires a minimum sample size of 35 nmol nitrate-N at Brown. (Note that $\Delta^{17}\text{O}$ and $\delta^{18}\text{O}$ are thus determined independently as separate injections result in $\Delta^{17}\text{O}$ calculated from the O_2 measurements compared to $\delta^{18}\text{O}$ determined from N_2O analysis.) The $1\sigma_p$ of standards and replicates is reported in Table 1. For samples that were not analyzed, $\Delta^{17}\text{O}$ was estimated based on the strong linear relationship with $\delta^{18}\text{O}$ that is observed in our data set (section 4.2). A difference within $\pm 8\%$ of the “true” sample $\Delta^{17}\text{O}$, which is greater than the largest residual in the regressions, influences the $\delta^{15}\text{N}$ results by less than the method

precision. For the snowpit, the same approach was taken to correct the data using 15 samples with sufficient volume remaining after having been analyzed for $\delta^{15}\text{N}$ and $\delta^{18}\text{O}$.

4. Results

4.1. Nitrate Concentration

It is well established that insoluble dust and major ion concentrations (e.g., NO_3^- , Cl^- , F^- , SO_4^{2-} , Ca^{2+} , K^+ , Na^+ , NH_4^+ , and Mg^{2+}) in ice cores from throughout the central Andes reflect the strong seasonality of precipitation in the region [Thompson et al., 1986, 1995, 1998, 2006, 2013]. Dry seasons are marked by high concentrations of both dust and ions due to elevated fluxes and minimal snowfall, while low concentrations during the wet season reflect muted deposition and high snow accumulation. Dating of annual layers in Andean cores primarily relies on counting of these seasonal cycles in dust and chemistry, including $[\text{NO}_3^-]$ in particular (see Thompson et al. [1995, 1998] for examples).

Table 2. Range and Total Sample Size (n) of QND30 and Snowpit $\delta^{15}\text{N}$, $\delta^{18}\text{O}$, and $\Delta^{17}\text{O}$ in ‰

	Minimum	Maximum	n
2011 Snowpit			
$\delta^{15}\text{N}$	-7.6	7.5	32
$\delta^{18}\text{O}$	45.7	67.7	32
$\Delta^{17}\text{O}$	17.3 (12.9 ^a)	22.9	15
Section I (0–12 m)			
$\delta^{15}\text{N}$	-9.6	4.5	111
$\delta^{18}\text{O}$	28.8	66.1	111
$\Delta^{17}\text{O}$	6.1	22.5	12
Section II (12–24 m)			
$\delta^{15}\text{N}$	-14.1	0.2	134
$\delta^{18}\text{O}$	23.6	55.0	134
$\Delta^{17}\text{O}$	9.1 (5.2 ^a)	20.1	46
Section III (24–30 m)			
$\delta^{15}\text{N}$	-13.3	0.0	77
$\delta^{18}\text{O}$	2.3	54.6	77
$\Delta^{17}\text{O}$	12.0	20.1	8
Total QND30			
$\delta^{15}\text{N}$	-14.1	4.5	322
$\delta^{18}\text{O}$	2.3	66.1	322
$\Delta^{17}\text{O}$	6.2 (5.2 ^a)	22.5	66

^aThese values show notable departures from their respective data sets (see sections 4.2 and 4.3 and Figures 6a and 6c).

QND30 exhibits strong variability in $[\text{NO}_3^-]$, ranging from 0.26 to 18.69 μM (16–1159 ppb NO_3^- ; Figure 2). Characteristic seasonal cycles are evident, particularly below 12 m (Figures 2 and 3). Above this depth, seasonality exists but appears dampened with $[\text{NO}_3^-]$ varying between 0.46 and 4.88 μM (29–303 ppb NO_3^-). Counting of the dry season $[\text{NO}_3^-]$ peaks places the bottom age of the record at ~1980. Concentrations in the 2011 snowpit span 0.14 to 9.44 μM (8–585 ppb NO_3^-) and represent one seasonal cycle, i.e., dry season 2010 to dry season 2011 (Figure 4 and Table 2).

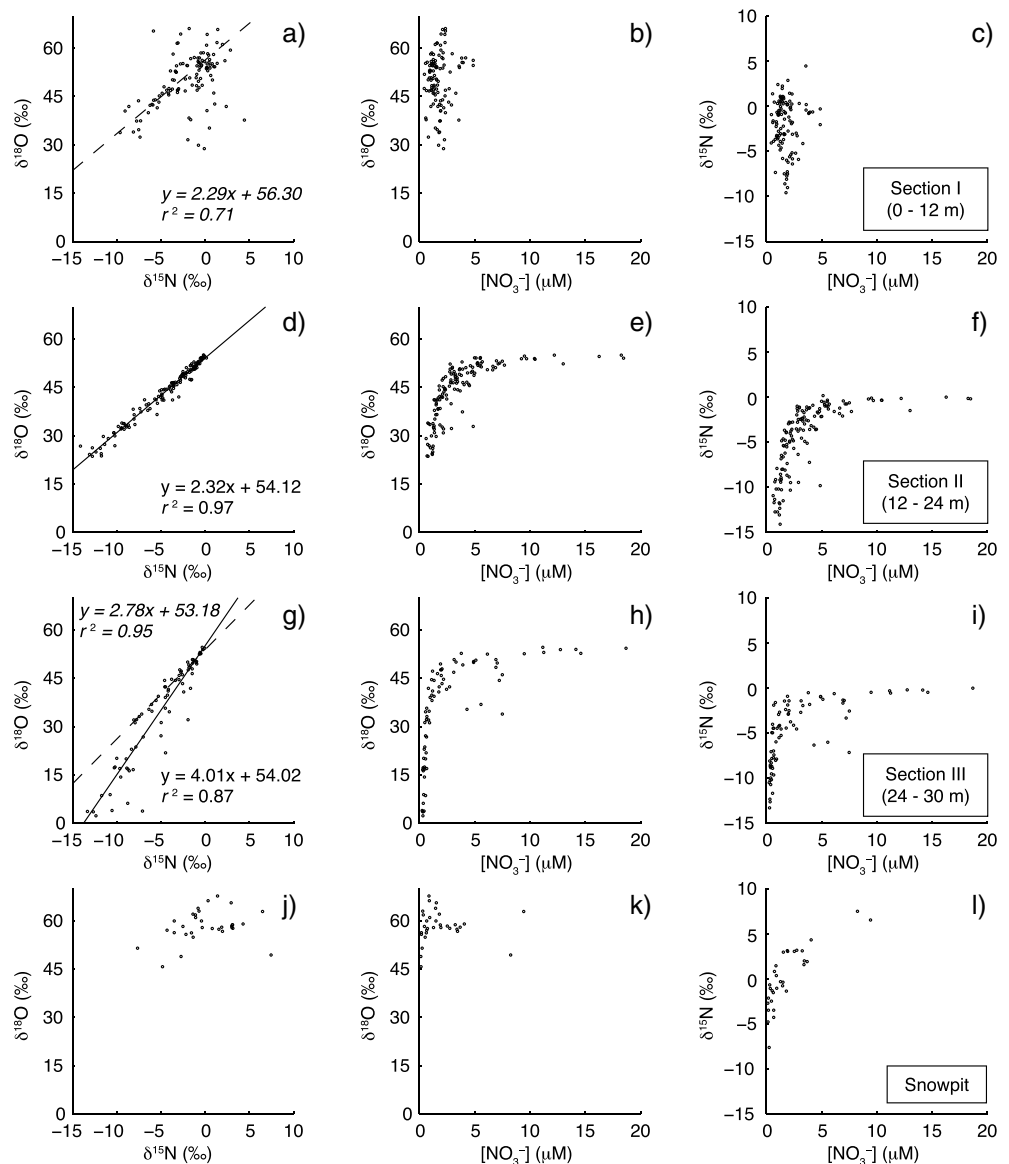


Figure 5. Plots of $\delta^{18}\text{O}$ versus $\delta^{15}\text{N}$, $\delta^{18}\text{O}$ versus $[\text{NO}_3^-]$, and $\delta^{15}\text{N}$ versus $[\text{NO}_3^-]$ for (a, b, c) Section I, (d, e, f) Section II, (g, h, i) Section III, and (j, k, l) the 2011 snowpit. Least squares regressions are noted with lines and are significant at $p < 0.001$. The solid lines in Figures 5d and 5g include all data. The dashed line in Figure 5a represents samples with $\delta^{15}\text{N} < -2\text{‰}$ and $\delta^{18}\text{O} < 54\text{‰}$ only. The dashed line in Figure 5g represents samples from 24.0–24.5 m and 26.0–28.8 m in Section III and thus excludes samples from intervals of extremely low $[\text{NO}_3^-]$. See Figure 2 and text for further discussion. Equations and r^2 values for the regressions marked with dashed lines are noted in italics.

4.2. QND30 Isotopic Composition

There are marked differences in $\delta^{15}\text{N}$, $\delta^{18}\text{O}$, and $\Delta^{17}\text{O}$ between sections of the core in terms of absolute values, seasonality, and how the three isotopic parameters relate to each other and to $[\text{NO}_3^-]$. To aid the discussion below, we thus segregate the results into three depth intervals: 0 to 12 m (Section I), 12 to 24 m (Section II), and 24 to 30 m (Section III).

4.2.1. Section I—0 to 12 m

Section I generally appears isotopically enriched relative to the record below (Figure 2 and Table 2). $\delta^{15}\text{N}$ and $\delta^{18}\text{O}$ vary from -9.6 to 4.5‰ and 28.8 to 66.1‰ , respectively, and these ranges include the highest values observed in QND30. It is interesting to note that enrichment in the top 12 m is much more apparent in the absence of the very low values found in the sections below. Section I also lacks straightforward variability in

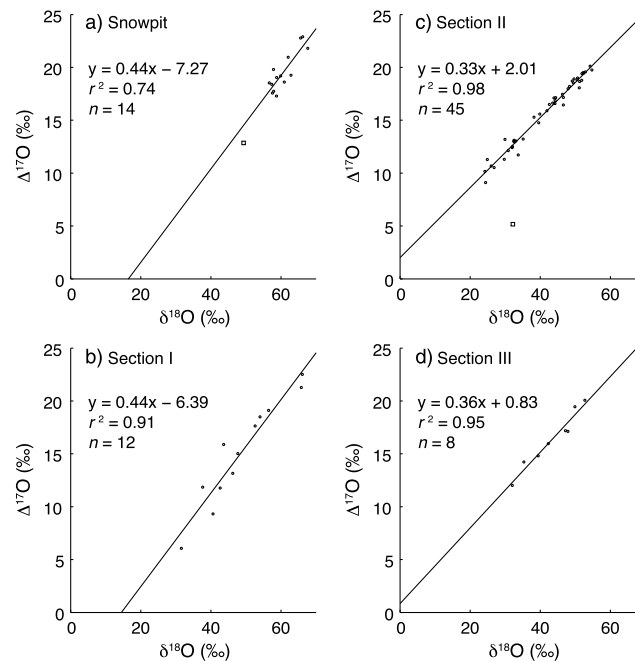


Figure 6. Snowpit and QND30 section plots of $\Delta^{17}\text{O}$ versus $\delta^{18}\text{O}$. Samples marked with open squares are influential values and are not included in the regressions. All regressions are significant at $p < 0.001$.

$\delta^{15}\text{N}$ and $\delta^{18}\text{O}$ unlike the lower core where there are defined seasonal cycles corresponding to $[\text{NO}_3^-]$. As noted above, $[\text{NO}_3^-]$ seasonality in this section is identifiable but appears muted. No clear relationship exists between $[\text{NO}_3^-]$ and $\delta^{15}\text{N}$ or $\delta^{18}\text{O}$ (Figures 5b and 5c). There is considerable spread in the data when $\delta^{18}\text{O}$ is plotted against $\delta^{15}\text{N}$, especially at higher values, though a linear relationship appears to exist for values of $\delta^{15}\text{N} < -2\text{‰}$ and $\delta^{18}\text{O} < 54\text{‰}$ (Figure 5a).

$\Delta^{17}\text{O}$ in the samples available from Section I varies between 6.1 and 22.5‰ (Table 2). Four of these samples possess $\Delta^{17}\text{O}$ compositions (21.1 to 22.9‰) that exceed the maximum value of 20.1‰ observed in the lower core. These samples are also characterized by $\delta^{18}\text{O}$ values above the range in Sections II and III. There is a strong linear relationship between $\Delta^{17}\text{O}$ and $\delta^{18}\text{O}$ (Figure 6b), but no correspondence exists with $\delta^{15}\text{N}$ or $[\text{NO}_3^-]$.

4.2.2. Section II—12 to 24 m

As with $[\text{NO}_3^-]$, isotopic seasonality is clearly identifiable below 12 m, with higher $\delta^{15}\text{N}$ and $\delta^{18}\text{O}$ corresponding to the increased $[\text{NO}_3^-]$ that marks dry seasons (Figures 2 and 3). Low isotope values accompany low $[\text{NO}_3^-]$ during wet seasons but are more variable. This is evident when $\delta^{15}\text{N}$ and $\delta^{18}\text{O}$ are plotted against $[\text{NO}_3^-]$ (Figures 5e and 5f). These relationships are nonlinear and seemingly approach constant values of 0 and 55‰ for $\delta^{15}\text{N}$ and $\delta^{18}\text{O}$, respectively, at concentrations above $\sim 5\ \mu\text{M}$. There is also a highly significant correspondence between $\delta^{18}\text{O}$ and $\delta^{15}\text{N}$ that approximates a line with endpoint coordinates—i.e., $(\delta^{15}\text{N}, \delta^{18}\text{O})$ in ‰—of roughly (0, 55) and (−13, 24) (Figure 5d). This regression is similar to that for the Section I samples with compositions of $\delta^{15}\text{N} < -2\text{‰}$ and $\delta^{18}\text{O} < 54\text{‰}$ (Figure 5a).

Section II samples measured for $\Delta^{17}\text{O}$ range between 5.2 and 20.1‰ (Table 2). As in Section I, there is a strong, linear $\Delta^{17}\text{O}$ versus $\delta^{18}\text{O}$ relationship but with a slope that is comparatively not as steep (Figure 6c). One sample with a noticeable departure (depth = 19.98 m; $\Delta^{17}\text{O} = 5.2\text{‰}$; $\delta^{18}\text{O} = 32.2\text{‰}$; $\delta^{15}\text{N} = -9.5\text{‰}$; $[\text{NO}_3^-] = 2.92\ \mu\text{M}$) is excluded from this calculation since the ordinary least squares method is not resistant to observations which exert excessive influence on the regression. $\Delta^{17}\text{O}$ is also linearly related to $\delta^{15}\text{N}$ in Section II and converges on a value of $\sim 20\text{‰}$ at higher concentrations when plotted against $[\text{NO}_3^-]$ (Figures S2 and S3).

4.2.3. Section III—24 to 30 m

Sections II and III are broadly similar but with key distinctions to be made between the two. As in Section II, isotopic seasonality exists below 24 m but is not as clearly defined, particularly in the lowermost 2 m of the core. The range in $\delta^{15}\text{N}$ is effectively equivalent to that in Section II as is the upper end of $\delta^{18}\text{O}$, i.e., during dry seasons (Figure 2 and Table 2). However, $\delta^{18}\text{O}$ is as much as 23‰ lower in Section III with a minimum of 2.3‰. When $\delta^{18}\text{O}$ is plotted against $\delta^{15}\text{N}$, the data exhibit more variance compared to Section II and are fit by a steeper regression (Figure 5g). Samples for which $\delta^{18}\text{O}$ is below the range in Section II fall within depth intervals also marked by very low $[\text{NO}_3^-]$ (24.5–26.0 and 28.8–30 m). These low- $\delta^{18}\text{O}$ samples, however, still appear part of a consistent and continuous nonlinear relationship with $[\text{NO}_3^-]$ (Figures 5h and 5i). Interestingly, samples that are not from these low- $[\text{NO}_3^-]$ intervals are characterized by a $\delta^{18}\text{O}$ versus $\delta^{15}\text{N}$ regression similar to that for Section II (Figure 5g).

Values for $\Delta^{17}\text{O}$ in Section III range between 12.0 and 20.1‰ and are linearly related to both $\delta^{18}\text{O}$ and $\delta^{15}\text{N}$ (Table 2 and Figures 6d and S2). The composition and character of these values are similar to those in Section II. This would seem to conflict with the different relationships between $\delta^{18}\text{O}$ and $\delta^{15}\text{N}$ in the two sections (Figures 6c and 6d). This apparent discrepancy is likely due to the fact that Section III sample availability was limited by volume, and samples with $[\text{NO}_3^-]$ less than 0.85 μM could not be analyzed. As a result, no samples with $\delta^{18}\text{O}$ below the range observed for Section II were measured for $\Delta^{17}\text{O}$, and those that were analyzed had isotopic compositions which plot close to the $\delta^{18}\text{O}$ versus $\delta^{15}\text{N}$ regression for Section II.

4.3. 2011 Snowpit

Snowpit $\delta^{15}\text{N}$ and $\delta^{18}\text{O}$ range from -7.6 to 7.5 ‰ and 45.7 to 67.7 ‰, respectively (Table 2). Like Section I, these values are generally higher than in Sections II and III, and seasonality is not apparent in isotopic composition despite being present in $[\text{NO}_3^-]$ (Figure 4). There is also little or no correspondence between $\delta^{18}\text{O}$, $\delta^{15}\text{N}$, and $[\text{NO}_3^-]$ (Figures 5j–5l). Snowpit $\Delta^{17}\text{O}$ varies between 12.9 and 22.9‰, but these measurements represent mostly dry season samples due to the limited volumes available for analysis. As with Section I, there is a linear relationship between $\Delta^{17}\text{O}$ and $\delta^{18}\text{O}$ that is steeper compared to Sections II and III (Figure 6a). One sample (depth = 0.02 m; $\Delta^{17}\text{O} = 12.9$ ‰; $\delta^{18}\text{O} = 49.4$ ‰; $\delta^{15}\text{N} = 7.5$ ‰; $[\text{NO}_3^-] = 8.26$ μM) is not included in the regression as it is a highly influential value. The snowpit is also similar to Section I in that there is no statistically significant relationship between $\Delta^{17}\text{O}$ and $\delta^{15}\text{N}$ (Figure S2a).

5. Discussion

Any interpretation of nitrate archived in ice must consider that it is not irreversibly deposited in the snowpack. Nitrate can be lost from the surface and near-surface via photolysis and/or evaporation of HNO_3 [Honrath *et al.*, 1999, 2000; Jones *et al.*, 2000; Röthlisberger *et al.*, 2000, 2002; Dibb *et al.*, 1998, 2002; Grannas *et al.*, 2007]. The extent of loss, however, is dependent on local factors such as snow accumulation rate, temperature, snow chemistry and pH, actinic flux, and the chemical form and physical state in which nitrate is present [Freyer *et al.*, 1996; Röthlisberger *et al.*, 2000, 2002; Burkhardt *et al.*, 2004, 2009; Grannas *et al.*, 2007].

Loss can be particularly severe at sites where accumulation rates are extremely low. At Dome C and Vostok in East Antarctica (< 10 cm snow yr^{-1} [Röthlisberger *et al.*, 2000]), decreases in $[\text{NO}_3^-]$ approaching 100-fold are observed over the top few centimeters of the snowpack [Mayewski and Legrand, 1990; Wagnon *et al.*, 1999; Röthlisberger *et al.*, 2000; Blunier *et al.*, 2005; Frey *et al.*, 2009]. Isotopic fractionation associated with such loss is striking. Decreasing $[\text{NO}_3^-]$ over the top 10 cm at Dome C, for example, is coincident with a ~ 200 ‰ increase in $\delta^{15}\text{N}$ attributed to the photolytic destruction of nitrate [Blunier *et al.*, 2005; Frey *et al.*, 2009]. Such change appears consistent with other sites on the East Antarctic Plateau [Erbland *et al.*, 2013].

Under higher accumulation regimes, however, seasonal and interannual profiles of $[\text{NO}_3^-]$ and isotopic composition appear largely preserved indicating that postdepositional alteration is less influential [Mulvaney and Wolff, 1993; Burkhardt *et al.*, 2004, 2006; Hastings *et al.*, 2004; Dibb *et al.*, 2007; Jarvis *et al.*, 2008, 2009]. This is evident at Summit, Greenland (~ 65 cm snow yr^{-1} [Dibb and Fahnstock, 2004]) where it is estimated that 70 to over 90% of deposited nitrate is preserved [Burkhardt *et al.*, 2004; Dibb *et al.*, 2007]. At the same site, Hastings *et al.* [2004] found no change in $[\text{NO}_3^-]$, $\delta^{15}\text{N}$, or $\delta^{18}\text{O}$ in overlapping snowpits sampled at the beginning and end of the summer, i.e., after 6 months of continuous irradiance. Modeling work by Jarvis *et al.* [2008] concluded that the seasonal profiles in these same snowpits could not be explained by photochemical processing.

In this context, the QIC presents an interesting case in that snow accumulation is roughly 3 to 5 times greater than at summit, but the distribution is strongly skewed toward the wet season. During the dry season, prolonged exposure of snow at the surface increases the potential for photolysis. Additionally, the relatively warm temperatures at the site may promote evaporation of HNO_3 . These possibilities must be considered before any attempt is made to interpret the downcore archive. In what follows, we evaluate the QND30 and 2011 snowpit records in terms of processes that can alter the isotopic composition and/or concentration of nitrate subsequent to its deposition. These include the direct and indirect effects of photolysis (section 5.1), evaporation (section 5.2), englacial microbial activity (section 5.3), and meltwater leaching (section 5.5).

5.1. Assessing Photolytic Alteration

5.1.1. Isotopic Fractionation of Nitrate by Photolysis

The major pathways for nitrate photolysis at Earth's surface proceed by



with reaction (R1) thought to be roughly 8 to 9 times more effective than (R2) [Warneck and Wurzinger, 1988; Dubowski et al., 2001]. These reactions are thought to take place in the aqueous phase within a quasi-liquid layer (QLL) on the surface of ice crystals, and yields measured in liquid and ice thus appear continuous across the freezing point [Dubowski et al., 2001; 2002; Chu and Anastasio, 2003; Grannas et al., 2007]. Nitrate photochemistry in snow is complex [e.g., Jacobi and Hilker, 2007; Abida and Osthoff, 2011], but losses under most conditions are expected to be as NO_2 and NO released in the gas phase from the QLL. NO_2 is primarily derived via (R1) or by the reaction of NO_2^- with OH , while NO is a product of NO_2^- and NO_2 photolysis. NO_2 can also be oxidized back to NO_3^- by OH at rates comparable to its transfer to the gas phase [Jacobi and Hilker, 2007]. Under acidic conditions ($\text{pH} < \sim 5$), the protonation of NO_2^- to form gaseous HONO is also important [Grannas et al., 2007, and references therein].

Frey et al. [2009] examined photolytic fractionation of nitrate in snow at Dome C using a theoretical framework first applied by Yung and Miller [1997] to stratospheric N_2O . The framework exploits mass-dependent differences in vibrational frequency and ground-state energy for a given set of isotopologues. These differences shift the spectral absorptivities of the heavier isotopologues to longer wavelengths and are, in turn, directly related to their isotopic fractionation constants [Miller and Yung, 2000]. As pointed out by Frey et al. [2009], this assumes that the different nitrate isotopologues retain similar spectral absorption curves and equal quantum yields. Despite these assumptions, we agree that this approach provides a useful first approximation with which to assess available observations.

The photolysis rate constant, j_A (s^{-1}), for a given molecule, A , can be calculated by

$$j_A = \int_{\lambda_1}^{\lambda_2} \sigma_A(\lambda, T) \phi_A(\lambda, T, \text{pH}) I(\lambda) d(\lambda), \quad (3)$$

where σ_A is the spectral absorptivity (cm^{-2}), I is the spectral actinic flux ($\text{photons cm}^{-2} \text{sec}^{-1} \text{nm}^{-1}$), and ϕ_A is the quantum yield and represents the probability (0 to 1) that dissociation occurs [Seinfeld and Pandis, 2006]. Using rate constants derived by integrating this equation for a given photolysis pathway and heavy/light isotopologue pair (e.g., ${}^{15}\text{N}{}^{16}\text{O}_3^- / {}^{14}\text{N}{}^{16}\text{O}_3^-$), an isotopic enrichment factor, ε (‰), can be calculated by

$$\varepsilon = \left(\frac{j_{\text{heavy}}}{j_{\text{light}}} - 1 \right) \cdot 10^3 = (\alpha - 1) \cdot 10^3, \quad (4)$$

where α is the fractionation constant in the classical Rayleigh equation [Criss, 1999]

$$\delta_{\text{residual}} = (\delta_{\text{initial}} + 10^3) \cdot f^{(\alpha-1)} - 10^3, \quad (5)$$

and f is the fraction of the initial nitrate pool remaining in the snowpack, i.e., $[\text{NO}_3^-]_{\text{residual}} / [\text{NO}_3^-]_{\text{initial}}$.

Given the predominance of reaction (R1), we have carried out the above calculations for this pathway using spectral absorptivities measured by Chu and Anastasio [2003] between 280 and 360 nm at 278°K. Measurements were made only between 278 and 298°K, but the authors note that σ varies little over this range. The quantum yield was calculated to be 5.57×10^{-3} at 273°K, and $\text{pH} = 5$ in the same study. The pH of QND30 samples is likely circumneutral to basic (section 5.4), but changes in ϕ at $\text{pH} \geq 5$ are negligible. A mean daily actinic flux ($\lambda = 280$ to 360 nm) at the QIC was estimated for each month of 2003 using the Tropospheric Ultraviolet Visible (TUV) 5.0 radiation model assuming clear sky conditions and includes total-column O_3 concentrations [Madronich and Flocke, 1998].

The resulting mean annual enrichment factors are $\varepsilon_{15\text{N}} = -42.5 \pm 0.9\text{‰}$ and $\varepsilon_{18\text{O}} = -30.5 \pm 0.6\text{‰}$. For comparison, Frey et al. [2009] calculated values for summer conditions at Dome C of $\varepsilon_{15\text{N}} = -47.6\text{‰}$ and $\varepsilon_{18\text{O}} = -34.2\text{‰}$. Monthly averages for the QIC vary from -41.7 to -44.1‰ for $\varepsilon_{15\text{N}}$ and -29.9 to -31.6‰ for

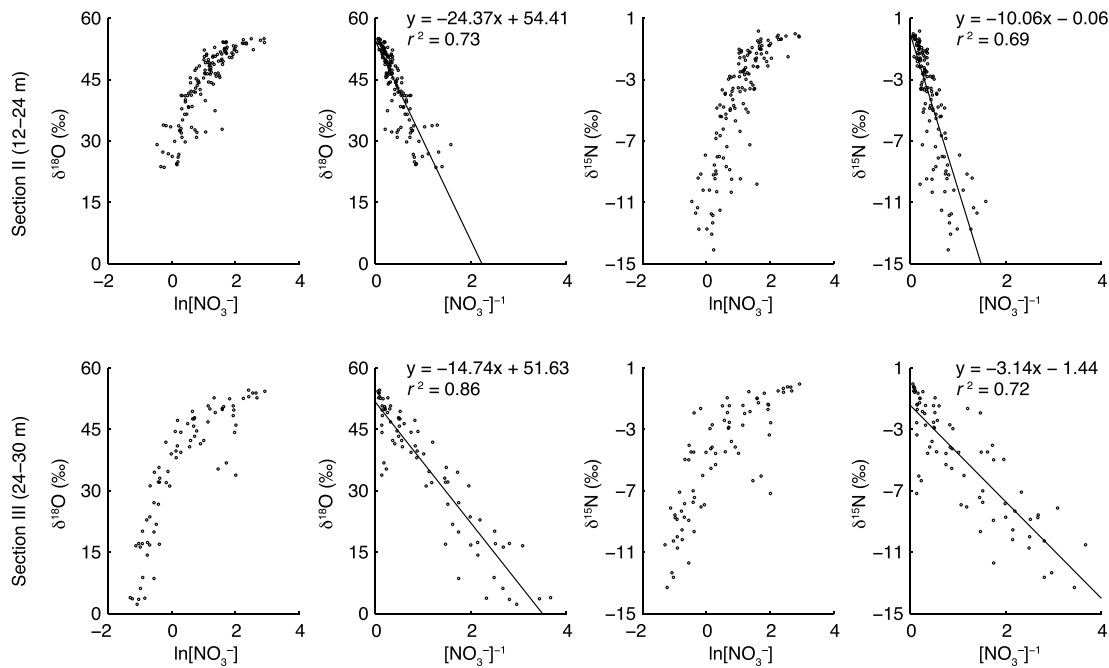


Figure 7. $\delta^{18}\text{O}$ and $\delta^{15}\text{N}$ versus $\ln[\text{NO}_3^-]$ and $[\text{NO}_3^-]^{-1}$ for Sections (top row) II and (bottom row) III. All regressions are significant at $p < 0.001$.

$\epsilon_{18\text{O}}$ with the more negative values centered around the month of June, i.e., the dry season. This implies that the fraction lost by photolysis will be isotopically depleted relative to the residual nitrate in the snow which, in turn, will undergo strong progressive enrichment. Additionally, increases in $\delta^{15}\text{N}$ will exceed those in $\delta^{18}\text{O}$ due to the more negative $\epsilon_{15\text{N}}$ value.

5.1.2. Photolysis—Direct Effects

We begin by assuming the null hypothesis that $\delta^{15}\text{N}$ and $\delta^{18}\text{O}$ variability in QND30 is, exclusively, controlled by photolytic fractionation following from the calculated enrichment factors. We assume that the initial nitrate pool is deposited at the surface with a fixed isotopic composition and concentration and that fractionation proceeds as a Rayleigh-type process such that it is unidirectional and enrichment is a function of the residual concentration. When using the approximate form of equation (5),

$$\delta_{\text{residual}} \approx \delta_{\text{initial}} + \epsilon \cdot \ln[\text{NO}_3^-]_{\text{residual}}, \quad (6)$$

it is clear that a regression of observed δ versus $\ln[\text{NO}_3^-]$ will be linear with a slope roughly equal to the enrichment factor [e.g., Mariotti *et al.*, 1988].

At Dome C, changes in $\delta^{15}\text{N}$ and $[\text{NO}_3^-]$ appear to be adequately described within this framework. There is strong, progressive enrichment as $[\text{NO}_3^-]$ decreases in the snowpack, and a regression of $\delta^{15}\text{N}$ versus $\ln[\text{NO}_3^-]$ is approximately linear with the derived ϵ values agreeing reasonably well with that modeled for photolysis at this site [Blunier *et al.*, 2005; Frey *et al.*, 2009].

With regard to QND30, there is no correspondence between the isotope parameters and $[\text{NO}_3^-]$ above 12 m (which we address in section 5.5), while $\delta^{15}\text{N}$ and $\delta^{18}\text{O}$ in Sections II and III exhibit nonlinear relationships with $[\text{NO}_3^-]$ as progressively higher values correspond with increasing $[\text{NO}_3^-]$ (Figure 5). This pattern is opposite that predicted by the modeled ϵ values since photolytic loss would lead to enrichment at lower concentrations. Additionally, $\delta^{15}\text{N}$ and $\delta^{18}\text{O}$ are not linearly related to $\ln[\text{NO}_3^-]$ and this further conflicts with a simple Rayleigh process.

It is important, however, to qualify this last point. Equation (5) requires that $[\text{NO}_3^-]_{\text{initial}}$ be fixed, but nitrate deposition at the QIC varies seasonally and is also concentrated at the surface during the dry season. With respect to Figure 7, higher dry season concentrations would increase $\ln[\text{NO}_3^-]$ corresponding to higher $\delta^{15}\text{N}$ and $\delta^{18}\text{O}$ in samples from these periods and obscure a linear relationship.

Still, the data from Sections II and III do not fit with the assumption of direct photolytic fractionation in three ways. First, there is virtually no change in $\delta^{15}\text{N}$ or $\delta^{18}\text{O}$ at high concentrations as is illustrated by plots of δ

versus $[\text{NO}_3^-]$ (Figures 5e, 5f, 5h, and 5i). This implies that any fractionating loss process must be negligible during the dry season because it is the *fraction* lost from an initial reactant pool that governs the degree of enrichment, not the initial concentration. Second, relative changes in $\delta^{15}\text{N}$ and $\delta^{18}\text{O}$ due to fractionation should vary predictably and proportionally to their enrichment factors regardless of changes in $[\text{NO}_3^-]_{\text{initial}}$. If driven by photolysis alone, a plot of $\delta^{18}\text{O}$ versus $\delta^{15}\text{N}$ would approximate a line with a slope of ~ 0.7 (i.e., $\epsilon_{18\text{O}}/\epsilon_{15\text{N}}$). Linear regressions of $\delta^{18}\text{O}$ versus $\delta^{15}\text{N}$ for Sections II and III, however, display slopes of 2.3 and 4.0, respectively (Figures 5d and 5g). Finally, photolytic fractionation would have no direct effect on $\Delta^{17}\text{O}$ since it is a mass-dependent process, yet $\Delta^{17}\text{O}$ clearly changes and exhibits strong relationships with $\delta^{18}\text{O}$ in all sections and with $\delta^{15}\text{N}$ in Sections II and III (Figures 6 and S2).

5.1.3. Photolysis—Secondary Oxidation Effects

As discussed above, direct photolytic loss should increase both $\delta^{15}\text{N}$ and $\delta^{18}\text{O}$ in the residual NO_3^- while leaving $\Delta^{17}\text{O}$ unaltered. In East Antarctic snowpit profiles, however, $\delta^{18}\text{O}$ and $\Delta^{17}\text{O}$ consistently show decreases with depth that are coincident with the strong $\delta^{15}\text{N}$ increases predicted by photolysis [Frey *et al.*, 2009; Erbland *et al.*, 2013]. One explanation for this apparent discrepancy is that the NO_2 , NO_2^- , and NO photolytic products undergo subsequent oxidation reactions with OH and H_2O in the QLL to produce secondary NO_3^- [McCabe *et al.*, 2005; Jacobi and Hilker, 2007]. Since OH and H_2O typically possess a $\Delta^{17}\text{O}$ of $\sim 0\text{‰}$ and $\delta^{18}\text{O}$ lower than that of the initial NO_3^- [Dubey *et al.*, 1997; Meijer and Li, 1998; Michalski *et al.*, 2011], the evolving nitrate-O pool will be diluted by mixing with the re-formed NO_3^- , acting to decrease both $\delta^{18}\text{O}$ and $\Delta^{17}\text{O}$. Direct oxygen exchange between NO_3^- and H_2O is negligible except at HNO_3 concentrations far higher than those found in natural snow [Bunton *et al.*, 1952].

Decreases in $\delta^{18}\text{O}$ due to mixing with secondary NO_3^- should be offset to some degree by the competing effect of direct photolytic enrichment. This direct effect, as mentioned above, was invoked to explain the 250 to 300‰ increases in $\delta^{15}\text{N}$ observed in East Antarctic snowpits [Frey *et al.*, 2009; Erbland *et al.*, 2013]. Following from the ratio of photolytic enrichment factors calculated by Frey *et al.* [2009] for Dome C ($\epsilon_{18\text{O}}/\epsilon_{15\text{N}}$), this would equate to concomitant increases in $\delta^{18}\text{O}$ of 180 to 216‰ due solely to direct photolytic loss. The observed changes in $\delta^{18}\text{O}$, which are on the order of -30 to -40‰ , imply that mixing with an isotopically depleted oxygen pool has been substantial.

Variations in $\delta^{15}\text{N}$ do not correspond to $\delta^{18}\text{O}$ or $\Delta^{17}\text{O}$ in Section I, but $\delta^{15}\text{N}$ changes in Sections II and III are of the same sign as $\delta^{18}\text{O}$ and $\Delta^{17}\text{O}$ (Figures 5, 6, and S2). This behavior in the lower sections suggests that secondary oxidation in the QLL has not been extensive. Even if it is assumed that increases in $\delta^{18}\text{O}$ are due to photolytic enrichment somehow outweighing secondary isotopic depletion, which seems unlikely following from the discussion of direct effects above, $\Delta^{17}\text{O}$ should still decrease if oxygen exchange was taking place with OH or H_2O (i.e., slopes of the $\Delta^{17}\text{O}$ versus $\delta^{18}\text{O}$ linear regressions would be negative) since $\Delta^{17}\text{O}$ would be unaffected by the mass-dependent fractionation.

NO_x can also be released from the QLL and react in the gas phase to form secondary nitrate within or above the snowpack. In East Antarctica, emissions of NO_x and nitrate from the interior can be transported by katabatic winds and redeposited along the coast [Savarino *et al.*, 2007]. Redeposition at the QIC, however, may be mitigated by several factors: snow on the ice cap should be well ventilated by wind pumping and convection driven by diurnal heating; the ice cap is small, measuring only about 3 to 14 km wide at its center (Figure S1); and the median hourly wind speed measured at the summit is 14.5 km hr^{-1} (25th to 75th percentile is 9.8 to 19.9 km hr^{-1}) (D. Hardy, personal communication, 2013). Taken together, it seems likely that NO_x and nitrate flushed from the snow would be rapidly removed from the site. If it is assumed that nitrate was in fact being redeposited and had an oxygen isotopic signature set locally by oxidation in the gas phase (see also section 5.6.1), a decrease in the $\delta^{18}\text{O}$ and $\Delta^{17}\text{O}$ of NO_3^- in the snow would probably still be observed given that rates of NO_2 loss from the QLL are thought to be comparable to oxidation back to NO_3^- within the condensed phase [Jacobi and Hilker, 2007]. Following from this, $\Delta^{17}\text{O}$ (or $\delta^{18}\text{O}$) should still have a negative relationship with $\delta^{15}\text{N}$ for anything less than 100% redeposition (in which case $\delta^{15}\text{N}$ would not change).

5.2. Evaporation

In addition to photolysis, evaporation of HNO_3 has been proposed as a postdepositional loss pathway for nitrate [Dibb *et al.*, 1998; Mulvaney *et al.*, 1998; Röthlisberger *et al.*, 2000; Erbland *et al.*, 2013]. Evaporation

must be considered at the QIC given that the solubility of HNO_3 in ice is low and its expulsion to grain surfaces is promoted by increasing temperature [Thibert and Dominé, 1998]. The extent and isotopic effects of this process in snow, however, are poorly understood. Sato *et al.* [2008] found no detectable evaporative loss from the surfaces of frozen 100 μM NaNO_3 solutions acidified to a pH of 4 at -6°C over the course of several days. Since evaporation proceeds only as HNO_3 , this was attributed to the high dissociation constant for HNO_3 as weaker acids were readily lost, and it was suggested that evaporation would be further inhibited under alkaline conditions. Negligible loss of nitrate in snow has also been observed in field and laboratory sublimation experiments ranging from a few days to 1 month in duration [Cragin and McGilvary, 1995; Ginot *et al.*, 2001]. In the field experiment of Ginot *et al.* [2001], nitrate behaved conservatively when in the presence of base cations (Ca^{2+} , Mg^{2+} , Na^+ , and K^+), while losses were severe when associated with H^+ .

The isotopic effects of evaporation also remain an open question. Based on theoretical calculations that assumed fractionation to be determined by the protonation of the NO_3^- isotopologues in the aqueous phase to form HNO_3 (as opposed to the equilibria of the liquid-vapor transfer), Frey *et al.* [2009] estimated HNO_3 evaporative enrichment factors of $\epsilon_{15\text{N}} = 14.2\text{‰}$ and $\epsilon_{18\text{O}} = 0.8\text{‰}$ at -33°C , with little change at lower temperatures. However, in a sublimation experiment conducted by Erbland *et al.* [2013] at Dome C, an $\epsilon_{15\text{N}}$ of $0.9 \pm 1.5\text{‰}$ was derived from observations at -30°C . This value decreased to -0.3 ± 1.2 and $-3.6 \pm 1.1\text{‰}$ at -20 and -10°C , respectively. No data regarding changes in $\delta^{18}\text{O}$ or $\Delta^{17}\text{O}$ were reported.

Following from the discussion of photolysis above, the relationships between $\delta^{15}\text{N}$ and $\delta^{18}\text{O}$ in Sections II and III are similarly unexplained by the evaporative ϵ values calculated by Frey *et al.* [2009] as are the relationships with relative changes in $[\text{NO}_3^-]$, especially during the dry season. As discussed in section 5.1.2., assessing the data by comparison with $\ln[\text{NO}_3^-]$ is complicated by seasonal changes in surface concentration.

These conclusions should be taken with a degree of caution, however, given that our current understanding of evaporative fractionation remains low—the discrepancies in $\epsilon_{15\text{N}}$ between Frey *et al.* [2009] and Erbland *et al.* [2013] have yet to be reconciled, and no observational estimates of $\epsilon_{18\text{O}}$ are available. Despite the uncertainty, we still note that evaporative fractionation would be mass-dependent and thus cannot explain the observed changes in $\Delta^{17}\text{O}$.

5.3. Englacial Microbial Activity

Englacial microbial processes—e.g., nitrification and/or denitrification—have been invoked to explain anomalous N_2O concentrations in both polar and tropical ice cores [Campen *et al.*, 2003; Miteva *et al.*, 2007]. Nitrification and denitrification have not been directly assessed at the QIC, but we consider their effects in the context of our data given that nitrate can be produced or consumed by such activity.

Denitrification should be inhibited by oxic conditions in snow and firn, but its presence should still be resolvable since $\delta^{18}\text{O}$ systematically varies with $\delta^{15}\text{N}$ as a result of the $\sim 1:2$ ratio of the respective enrichment factors [Lehmann *et al.*, 2003; Kendall *et al.*, 2007]. This ratio predicts that increases in $\delta^{18}\text{O}$ relative to $\delta^{15}\text{N}$ in the residual nitrate will approximate a line with a slope of ~ 0.5 and which is invariant to changes in the initial $[\text{NO}_3^-]$. In contrast, regression slopes for $\delta^{18}\text{O}$ versus $\delta^{15}\text{N}$ in Sections II and III are 2.3 and 4.0, respectively (Figures 5d and 5g). Furthermore, denitrification is a mass-dependent process and would leave $\Delta^{17}\text{O}$ unchanged.

Unlike denitrification, nitrification produces NO_3^- ($\text{NO}_{3\text{nitrif}}^-$) with nitrogen and oxygen derived from different sources. Nitrogen originates from ammonium (NH_4^+) but is subject to fractionation during conversion. Culture studies suggest that the $\delta^{15}\text{N}$ of $\text{NO}_{3\text{nitrif}}^-$ ($\delta^{15}\text{N}_{\text{nitrif}}$) should be offset by at least -14 to -38‰ relative to that of NH_4^+ [Kendall *et al.*, 2007, and references therein]. If the initial NH_4^+ pool is finite, however, the $\delta^{15}\text{N}$ of the accumulating $\text{NO}_{3\text{nitrif}}^-$ will approach that of NH_4^+ as the reactant is consumed.

Oxygen in $\text{NO}_{3\text{nitrif}}^-$ is typically interpreted as a mixture of one atom from ambient atmospheric O_2 ($\delta^{18}\text{O}_{\text{atm}}$) and two from the surrounding water:

$$\delta^{18}\text{O}_{\text{nitrif}} = (1/3) \cdot \delta^{18}\text{O}_{\text{atm}} + (2/3) \cdot \delta^{18}\text{O}_{\text{water}}, \quad (7)$$

where $\delta^{18}\text{O}_{\text{atm}}$ is 23.88‰ [Barkan and Luz, 2005] and $\delta^{18}\text{O}_{\text{water}}$ can be approximated as that of QIC snow (melting is effectively nonfractionating), which varies from roughly -28 to -10‰ between wet and dry seasons, respectively. $\Delta^{17}\text{O}_{\text{nitrif}}$ will equal that of O_2 and H_2O , which are $\sim 0\text{‰}$.

Estimates for $\delta^{18}\text{O}_{\text{nitrif}}$ are thus between -11 and 1‰ depending on the seasonal snow composition. These values are far lower than observed $\delta^{18}\text{O}$ in the dry season (i.e., high $[\text{NO}_3^-]$ samples with $\delta^{18}\text{O}$ up to $\sim 55\text{‰}$), but this does not rule out the possibility that lower $\delta^{18}\text{O}$ during wet seasons is due to nitrification having diluted a dry season input via mixing. This nominally fits with the $\Delta^{17}\text{O}$ versus $\delta^{18}\text{O}$ regression for Section II since the x intercept of -6‰ could be interpreted as the $\delta^{18}\text{O}_{\text{nitrif}}$ end-member (since $\Delta^{17}\text{O}_{\text{nitrif}}$ is 0‰ , corresponding to O_2 and H_2O ; Figure 6c) and is within the estimated range. If a $\delta^{18}\text{O}$ of 55‰ is taken as the dry season atmospheric end-member (Figure 5e and section 5.6), then $\delta^{18}\text{O}$ as low as 24‰ in Section II requires as much as 51% of the NO_3^- to be derived from in situ nitrification. This should also affect $\delta^{15}\text{N}$ such that, for a dry season end-member composition of 0‰ (Figure 5f) and the same 51% contribution from nitrification, a $\delta^{15}\text{N}_{\text{nitrif}}$ of -25‰ is needed to produce low $\delta^{15}\text{N}$ values of -13‰ (i.e., corresponding to $\delta^{18}\text{O} = 24\text{‰}$ via Figure 5d). Future measurements of the $\delta^{15}\text{N}$ of NH_4^+ are needed to evaluate whether such a $\delta^{15}\text{N}$ for $\text{NO}_3^-_{\text{nitrif}}$ is realistic.

Amoroso et al. [2010] presented evidence for nitrification in Arctic snow based in part on very high NO_2^- concentrations (1 to 10 μM) that were preserved by alkaline conditions in the snow. Identifying nitrification based on the presence of NO_2^- is complicated since the conversion of NO_2^- to NO_3^- is often not rate-limiting, but NO_2^- can accumulate when oxidation to NO_3^- is inhibited by high pH [*Shen et al.*, 2003] or NO_2^- consumption is otherwise decoupled from its production [*Ward*, 1996]. As noted above, $[\text{NO}_2^-]$ was not detected in QND30 or the snowpit. Major ion concentrations measured in two other cores drilled from the north and summit domes in 2003 suggest that QND30 is likely alkaline throughout and that $[\text{NH}_4^+]$ generally exceeds $[\text{NO}_3^-]$, especially during the wet season (section 5.4). Thus, it is possible that NO_2^- would be present in our samples if nitrification had been active.

Sections II and III are characterized by similar $\Delta^{17}\text{O}$ versus $\delta^{18}\text{O}$ regressions—resulting in $\delta^{18}\text{O}_{\text{nitrif}}$ estimates of -6 and -2‰ , respectively—though no samples with $\delta^{18}\text{O}$ below 32‰ in Section III were analyzed for $\Delta^{17}\text{O}$ due to insufficient volume (Figures 6c and 6d). The two $\delta^{18}\text{O}$ versus $\delta^{15}\text{N}$ regressions are also similar when excluding the data from the low- $[\text{NO}_3^-]$ intervals in Section III, which are also marked by very low $\delta^{18}\text{O}$ (24.5–26.0 and 28.8–30 m; Figures 5d and 5g). To explain such low $\delta^{18}\text{O}$ values (approaching 2‰) in Section III would require an 87% contribution from nitrification using the same assumed values above, yet the range in $\delta^{15}\text{N}$ is very similar for the two sections. As such, it is unlikely that the compositions of these intervals can be explained by a higher proportion of nitrate derived from in situ nitrification.

5.4. Possible Factors Mitigating Loss

We address the possibility that alteration has influenced the upper core and snowpit in section 5.5, but following from the discussion above, there appears to have been limited photolytic or evaporative alteration of QND30 below ~ 12 m. This conclusion seems surprising and especially so during the dry season when the residence time of nitrate at the surface would be relatively long.

The intensity of photolysis is directly related to light penetration in the snowpack. Typical e -folding depths—the depth at which the actinic flux has been attenuated by a factor of $1/e$ (~ 0.37)—for wavelengths at which nitrate photolyzes range between 5 and 25 cm but vary with solar zenith angle, snow density, grain size and shape, and impurity content (e.g., mineral dust, black carbon, and humic-like substances) [*Grannas et al.*, 2007; *France et al.*, 2011; *Zatko et al.*, 2013]. Concentrations of insoluble dust, pollen, charcoal, and other organics (including vegetation and insect fragments) in QIC snow can exceed those at polar sites by several orders of magnitude, especially during the dry season [*Thompson et al.*, 1979; *Thompson and Mosley-Thompson*, 1982; *Reese and Liu*, 2002; *Kehrwald et al.*, 2008]. One possibility then is that the effects of strong insolation and low solar zenith angles at the QIC have been offset to a degree by the significant impurity content in the snowpack, though this remains to be confirmed by in situ measurements of light penetration.

The extent of photolytic and evaporative loss is also influenced by snow chemistry. Several studies have proposed that nitrate in alkaline snow is likely to be less labile or even inert [*Thibert and Dominé*, 1998; *Legrand et al.*, 1999; *Ginot et al.*, 2001; *Röthlisberger et al.*, 2000, 2002; *Beine et al.*, 2002, 2003, 2006; *Amoroso et al.*, 2006; *Abida and Osthoff*, 2011]. Under such conditions, stable salts (e.g., $\text{Ca}(\text{NO}_3)_2$, $\text{Mg}(\text{NO}_3)_2$, or NaNO_3) may act to sequester NO_3^- in particulates or provide counter cations which stabilize NO_3^- in the liquid phase and inhibit evaporation as HNO_3 . Additionally, nitrate is more vulnerable to loss when present on grain surfaces, but

diffusivity in ice has only been measured for HNO_3 and may be orders of magnitude slower if associated with heavy cations [Thibert and Dominé, 1998], while the presence of NH_4^+ can promote incorporation of NO_3^- into the ice lattice [Gross and Svec, 1997; Eichler et al., 2001].

Major ion concentrations other than nitrate were not measured in QND30 but have been analyzed in two other cores drilled by the BPRC at the north and summit domes in 2003 (data not shown). Negative ion balances ($[\text{F}^- + \text{Cl}^- + \text{NO}_3^- + 2(\text{SO}_4^{2-})] - [2(\text{Ca}^{2+}) + \text{K}^+ + \text{Na}^+ + \text{NH}_4^+ + 2(\text{Mg}^{2+})]$ in $\mu\text{eq L}^{-1}$) throughout the top 30 m of these cores indicate alkaline conditions. Of the cations measured, Na^+ and NH_4^+ are the most abundant with $\text{Na}^+/\text{NO}_3^-$ and $\text{NH}_4^+/\text{NO}_3^-$ molar ratios consistently above 1. $\text{Na}^+/\text{NO}_3^-$ is generally higher during dry seasons, while $\text{NH}_4^+/\text{NO}_3^-$ is greater during wet seasons. Molar ratios relative to NO_3^- for all other cations are typically below 1 in both seasons. Given the close proximity of the three cores and the flat surface topography of the ice cap (Figure S1), these conditions should be representative of QND30 and imply the likelihood of nitrate being present as a stable salt.

5.5. Recent Melting

The 2011 snowpit and Section I are clearly distinct from the lower core in several ways which make it difficult to evaluate alteration in a manner similar to that for Sections II and III: there are no straightforward relationships between $\delta^{15}\text{N}$ and $\delta^{18}\text{O}$ or $\Delta^{17}\text{O}$ in Section I and the snowpit; the isotope parameters do not appear to relate to $[\text{NO}_3^-]$; $\delta^{15}\text{N}$ and $\delta^{18}\text{O}$ are higher on average compared to Sections II and III, especially in terms of wet season values; isotopic seasonality is not readily apparent; and $[\text{NO}_3^-]$ is lower on average while seasonal cycles, although present, are muted.

Such differences are not conclusive evidence for alteration, but taken together they do reflect a different regime, whether it be predepositional or postdepositional, under which the more recent record has formed. (Section I covers the period ~1997 to 2003 based on counting of the seasonal $[\text{NO}_3^-]$ peaks. The snowpit represents 1 year of snowfall.) Postdepositional changes are especially worth considering given the current anomalous climate regime at the QIC. Recent retreat of the ice cap due to warming has been dramatic and nonlinear [Thompson et al., 2006; Bradley et al., 2009], and ^{14}C dating of relict vegetation exposed at the margins since circa 2002 confirms that the QIC is smaller now than it has been in over 6000 years [Thompson et al., 2006, 2013; Buffen et al., 2009].

Recent warming has increased surface melt even at the summit and especially during the wet season when higher humidity and temperature promote ablation by melting over sublimation [Thompson et al., 2006]. Meltwater percolating along grain boundaries can leach major ions resulting in lower concentrations and smoothed seasonality [Davies et al., 1982; Eichler et al., 2001; Ginot et al., 2010]. Nitrate is vulnerable to elution, but such studies show varying degrees of removal since leaching rates are influenced by factors such as ion interactions [Eichler et al., 2001].

Leaching and consequent mixing of nitrate is consistent with lower $[\text{NO}_3^-]$ and smoothed profiles in Section I and the snowpit, as well as the lack of relationships between $[\text{NO}_3^-]$ and the isotope values. The preservation of seasonal $[\text{NO}_3^-]$ cycles below 12 m along with the absence of obvious melt features such as elongated vertical cavities or bubble-free ice [e.g., Thompson et al., 2009] suggests that the lower sections have not received percolation from above. Leaching alone, however, cannot explain $\delta^{15}\text{N}$ and $\delta^{18}\text{O}$ values in Section I and the snowpit that are above the ranges found in the lower core or the lack of correspondence between $\delta^{15}\text{N}$, $\delta^{18}\text{O}$, and $\Delta^{17}\text{O}$ as observed in Sections II and III if we consider that the isotopic compositions might otherwise be similar—which would explain why some samples from Sections I and III appear to fall along the $\delta^{18}\text{O}$ versus $\delta^{15}\text{N}$ regression for Section II (Figures 5a, 5d, and 5g). For example, if discrete samples from Section II were to be mixed, the resulting values would still place along the original $\delta^{18}\text{O}$ versus $\delta^{15}\text{N}$ regression in Figure 5d due to mass balance.

This suggests that if alteration of Section I and the snowpit has occurred, it must have been isotopically fractionating. As described in section 5.2, nitrate may be less prone to loss under alkaline conditions. Leaching, however, would likely raise the potential for loss via photolysis and/or evaporation since nitrate would be increasingly present in liquid and also undergo separation from other ions given the varied elution rates [Eichler et al., 2001]. Furthermore, H^+ has also been shown to be mobile and may accompany NO_3^- and SO_4^{2-} [Davies et al., 1982]. This would be consistent with snowpit pH measurements, which varied from ~7–8 in dry season

samples at the top of the profile to ~5 in wet season snow. Samples near the surface, however, should not necessarily be taken to represent pristine deposition given that they were exposed during the 2011 dry season prior to collection. Ultimately, concurrent collections of atmospheric samples, fresh and aged surface snow, and snowpit samples are needed to address whether or not alteration is presently occurring.

The two intervals of very low $[\text{NO}_3^-]$ in Section III (24.5 to 26.0 m and 28.8 to 30 m; Figure 2) are unusual compared to the rest of the record, and we question whether meltwater and leaching could explain these low concentrations. Percolation from directly above would seem unlikely given that the intervals in Section III are clearly defined and abruptly bounded by sections with seasonality in both isotopic composition and $[\text{NO}_3^-]$. Lateral transport, however, is possible along impermeable boundaries such as those within the transition from firn to ice [Eichler *et al.*, 2001]. These low- $[\text{NO}_3^-]$ intervals are located within the firn-ice transition, and meltwater at similar depths was observed pooling in the borehole during drilling of the 2003 summit dome core.

The isotopic composition of these intervals, however, is very different compared to Section I and the snowpit. There are no $\delta^{15}\text{N}$ or $\delta^{18}\text{O}$ values higher than those found in Section II, and while $\delta^{15}\text{N}$ is within a similar range, $\delta^{18}\text{O}$ values below the minimum found in Section II (23.6‰) are observed and extend to as low as 2.3‰ (Figures 5d and 5g). Additionally, $\delta^{15}\text{N}$ and $\delta^{18}\text{O}$ exhibit consistent nonlinear relationships with $[\text{NO}_3^-]$ (Figure 5). If the character of the upper core and snowpit were the result of elution having facilitated fractionation by photolysis or evaporation, these processes would be unable to affect sections far below the surface. The presence of very low $\delta^{18}\text{O}$ in Section III may thus reflect mixing with an isotopically depleted source of oxygen, but the nature of such a pool and process responsible is unclear.

5.6. Mixing of Atmospheric Nitrate

While it is possible that the snowpit and portions of QND30 have been affected by melting, it does not appear that photolysis or evaporation has significantly influenced the QND30 record below 12 m given our current understanding of these processes. This would then argue that either (a) our current estimates for photolytic and evaporative enrichment factors are incorrect; (b) additional photolysis pathways or other mechanisms of postdepositional alteration must be invoked but, if fractionating, must still be negligible during the dry season for Sections II and III; or (c) the isotopic composition of the nitrate input is variable and the relationships between $\delta^{15}\text{N}$, $\delta^{18}\text{O}$, and $\Delta^{17}\text{O}$ are determined prior to deposition (i.e., at the NO_x source or in the atmosphere).

Both fractionation and mixing of two sources with discrete isotopic compositions can produce similar but fundamentally different nonlinear relationships between $[\text{NO}_3^-]$ and $\delta^{15}\text{N}$ or $\delta^{18}\text{O}$ [Mariotti *et al.*, 1988; Kendall *et al.*, 2007]. Rayleigh fractionation proceeds such that linearity exists between δ and $\ln[\text{NO}_3^-]$ for a fixed initial concentration. Mixing, on the other hand, is governed by mass balance and results in linear relationships when δ is plotted against $[\text{NO}_3^-]^{-1}$. Plots of δ versus δ will also be linear and describe mixing lines that fall between the compositions of the two end-members. Such relationships between $\Delta^{17}\text{O}$ and $\delta^{18}\text{O}$ in nitrate have been interpreted in this context since $\Delta^{17}\text{O}$ is not directly altered by mass-dependent fractionation but will vary in proportion to mixing of different oxygen sources [Michalski *et al.*, 2003, 2004a, 2004b, 2005; Kendall *et al.*, 2007; Morin *et al.*, 2008].

The linear relationships between the isotopic parameters and with $[\text{NO}_3^-]^{-1}$ in Sections II and III would fit with mixing of two sources that vary seasonally (Figures 7 and S3). The approximate end-member composition of the nitrate input during the dry season would appear to be $\delta^{15}\text{N} = 0\text{‰}$, $\delta^{18}\text{O} = 55\text{‰}$, and $\Delta^{17}\text{O} = 20\text{‰}$ for both sections. Indeed, this end-member composition remains constant even with increasing $[\text{NO}_3^-]$ (Figures 5e, 5f, S2, and S3). The wet season component for Section II would be $\delta^{15}\text{N} = -13\text{‰}$, $\delta^{18}\text{O} = 24\text{‰}$, and $\Delta^{17}\text{O} = 10\text{‰}$ or less. In contrast to the dry season end-member, the isotope values at low $[\text{NO}_3^-]$ do not converge on a single composition and the quantification of this end-member should therefore be taken as a maximum estimate. Wet season values from the low- $[\text{NO}_3^-]$ intervals in Section III extend to $\delta^{15}\text{N} = -13\text{‰}$ and $\delta^{18}\text{O} = 2\text{‰}$, while those in the remainder of the section extend to $\delta^{15}\text{N} = -8\text{‰}$ and $\delta^{18}\text{O} = 31\text{‰}$. Section III $\Delta^{17}\text{O}$ is as low as 12‰ and seems to follow along a $\Delta^{17}\text{O}$ versus $\delta^{18}\text{O}$ regression similar to that for Section II (Figures 6c and 6d), but we note again that no samples with $\delta^{18}\text{O}$ lower than that observed in Section II were measured. Given the strong relationships between the two parameters, it seems reasonable that lower $\Delta^{17}\text{O}$ would also correspond to these

samples. To simplify an interpretation of these compositions, we address $\delta^{18}\text{O}$ and $\Delta^{17}\text{O}$ separately from $\delta^{15}\text{N}$ in the discussion below.

5.6.1. $\delta^{18}\text{O}$ and $\Delta^{17}\text{O}$

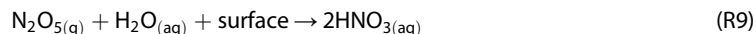
Atmospheric nitrate can be formed via several different chemical pathways. Production is initiated by oxidation of NO to NO_2 by either O_3 (R3) or peroxy radicals (HO_2 or RO_2) formed by reaction of a hydrogen atom or an organic radical (R) with O_2 ((R4) and (R5)).



In the presence of sunlight, the primary HNO_3 formation pathway is reaction of NO_2 with OH and an unreactive third body (M) such as N_2 (R6):



Production of HNO_3 also occurs via hydrolysis of dinitrogen pentoxide (N_2O_5) on an aerosol surface ((R7), (R8), and (R9)) or hydrogen abstraction by the nitrate radical (NO_3) from a hydrocarbon (HC) or dimethyl sulfide (DMS) (R10).



These pathways are restricted during the day due to photolysis of NO_3 and N_2O_5 and are also more prevalent in cold environments since N_2O_5 is thermally unstable as well.

The $\Delta^{17}\text{O}$ anomaly in atmospheric nitrate is derived from O_3 via reactions (R3) and (R7). In polar regions, reactive bromine (BrO) can also impart a high $\Delta^{17}\text{O}$ signature due to the role of O_3 in BrO formation [Morin *et al.*, 2012]. The $\Delta^{17}\text{O}$ of O_3 has been observed within the range 20 to 40‰ [Vicars *et al.*, 2012, and references therein], while that of the other oxidants is close to 0‰ [Alexander *et al.*, 2009; Morin *et al.*, 2011, and references therein]. The $\delta^{18}\text{O}$ of O_3 is also large, and measurements vary between 95 and 130‰ [Michalski *et al.*, 2011, and references therein].

Nitrate with nonzero $\Delta^{17}\text{O}$ is thus considered atmospheric in origin, with $\Delta^{17}\text{O}$ and $\delta^{18}\text{O}$ varying as a function of the fractional contribution of the reaction pathways above. Previous observations for $\delta^{18}\text{O}$ and $\Delta^{17}\text{O}$ range from roughly 25 to 115‰ and 10 to 45‰, respectively, and tend to vary with season and latitude [Alexander *et al.*, 2009; Michalski *et al.*, 2011, and references therein].

With regard to the tropics, nitrate production should be dominated by the reaction of NO_2 with OH (R6) following from the high temperatures, humidities, and insolation in these regions. This is in accord with the estimates of Alexander *et al.* [2009] from the GEOS-Chem global atmospheric chemistry model which predict that up to ~87% of atmospheric nitrate is formed by this pathway at low latitudes. In the same study, mean annual $\Delta^{17}\text{O}$ values as low as 7‰ are calculated at the surface over tropical forests due to increased NO_x cycling by peroxy radicals ((R4) and (R5)).

For the gridbox occupied by the QIC, the GEOS-Chem model estimates 3 month averages for $\Delta^{17}\text{O}$ in atmospheric nitrate of 20.6‰ (June-July-August); 21.0‰ (September-October-November); 11.5‰ (December-January-February), and 12.3‰ (March-April-May), with an annual mean of 19.2‰ (B. Alexander, personal communication, 2012). These predictions agree well with dry season $\Delta^{17}\text{O}$ (~20‰) in all sections of QND30 and with wet season values in Section II (~10‰) (Table 2 and Figure 6). In comparison with existing observations from the tropics, the $\Delta^{17}\text{O}$ of nitrate in fog water from the Podocarpus National Forest, Ecuador, was measured between 13 and 22‰ [Brothers *et al.*, 2008]. Bulk aerosols collected in the eastern tropical Atlantic boundary layer were observed to be within 22 to 30‰ [Morin *et al.*, 2009; Alexander *et al.*, 2009 and supporting information therein]. The $\Delta^{17}\text{O}$ of nitrate salts in the Atacama Desert, Chile, range between 14 and 21‰, but these deposits have accumulated over several million years and are thus not directly comparable.

The seasonal $\Delta^{17}\text{O}$ variability in QND30 can be explained within the context of regional atmospheric circulation patterns (Figure 1 and section 2). During the wet season, transport to the QIC is dominated by the entrainment of low-level air from the Amazon Basin onto the Altiplano by upper level easterly winds. This would be consistent with an increase in the relative contribution of peroxy radicals in the cycling of NO_x ((R3) and (R4)) and OH in the production of HNO_3 (R6). The reversal of wind direction aloft during the dry season results in westerly to northerly transport of midlevel air masses with colder and drier origins. These conditions would favor oxidation of NO by O_3 (R3) and nitrate formation via N_2O_5 hydrolysis ((R7), (R8), and (R9)), both resulting in higher $\Delta^{17}\text{O}$. The movement of low-level air onto the Altiplano during this season is restricted by coastal topography and atmospheric stability over the eastern Pacific due to coastal upwelling and descending Walker Circulation.

The $\Delta^{17}\text{O}$ of QND30 nitrate thus confirms an atmospheric origin. Seasonal variations are consistent with model predictions and regional circulation patterns, and atmospheric oxidation chemistry therefore provides an alternative explanation to mixing with an in situ nitrification source. The GEOS-Chem model does not calculate $\delta^{18}\text{O}$ explicitly, but most values in the core and snowpit fall within the range of previous atmospheric nitrate observations, which vary from 25 to 115‰ [Michalski *et al.*, 2011]. The exception to this would be $\delta^{18}\text{O}$ values approaching 2‰ in the low- $[\text{NO}_3^-]$ intervals of Section III, which remain unexplained.

5.6.2. $\delta^{15}\text{N}$

Unlike oxygen, the nitrogen atom can be conserved during the conversion of NO_x to nitrate. This has led to an interpretation of $\delta^{15}\text{N}$ as indicative of the precursor NO_x source. However, $\delta^{15}\text{N}$ may be influenced by fractionation during the cycling of NO_x , the conversion of NO_2 to nitrate, transport, or the formation of particulates.

Early work by *Begun and Melton* [1956] suggested that equilibrium fractionation during NO_x cycling leads to a 28‰ increase in the $\delta^{15}\text{N}$ of NO_2 relative to NO at 25°C. At low NO_x concentrations, there should be complete conversion such that the $\delta^{15}\text{N}$ of NO_2 would equal that of mean NO_x . *Freyer et al.* [1993], however, suggested that in environments where NO_x concentrations are high and exceed those of oxidants, incomplete conversion leads to a higher $\delta^{15}\text{N}$ in NO_2 that is then carried over to nitrate. This explanation was given to account for seasonal offsets between the $\delta^{15}\text{N}$ of gaseous HNO_3 and particulate nitrate at a polluted urban site in Jülich, Germany.

Unlike polluted environments, low NO_x concentrations are expected at the QIC given the remote location, but elevated NO_x (and O_3) mixing ratios occur in biomass burning plumes over the Amazon [*Andreae et al.*, 1988]. Burning is more prevalent during the dry season (when higher $\delta^{15}\text{N}$ is observed) and peaks in September and October, i.e., at the end of the dry season, but varies year to year [*Potter et al.*, 2002; *van der Werf et al.*, 2004]. Given the general consistency in $\delta^{15}\text{N}$ between, and within, dry seasons, we do not believe that incomplete conversion to NO_2 can explain our results.

Based on theoretical calculations, *Freyer* [1991] proposed that the $\delta^{15}\text{N}$ of nitrate produced by reaction (R6) should be offset by roughly -3% compared to NO_2 . This has been disputed by *Morin et al.* [2009], and given the lack of observational support, the potential fractionation is generally assumed to be negligible.

The possibility of isotope effects during atmospheric transport represents a longstanding question that remains unresolved. In the study by *Freyer* [1991], the $\delta^{15}\text{N}$ of particulate nitrate exceeded that in rainwater by $\sim 9\%$ throughout the year at Jülich. This was interpreted as a rainout effect such that wet deposition during transport led to progressive isotopic enrichment in the remaining nitrate. As noted by *Morin et al.* [2009], this reasoning has been invoked by a number of studies to rule out transport effects in explaining low $\delta^{15}\text{N}$ values observed in remote regions. The conclusions of *Freyer* [1991], however, conflict with observations from the eastern tropical Atlantic of higher $\delta^{15}\text{N}$ in rainwater compared to dry deposition [*Baker et al.*, 2007; *Morin et al.*, 2009].

In QND30, higher $\delta^{15}\text{N}$ during the dry season is unlikely to be the result of washout since precipitation is so limited and the observed values so consistent. Lower and more variable $\delta^{15}\text{N}$ during the wet season conflicts with the predictions of *Freyer* [1991] that wet deposition leads to progressive enrichment, but the wet season $\delta^{15}\text{N}$ would be consistent with washout should the observations of *Baker et al.* [2007] prove representative of precipitation effects. However, only two rainwater samples were collected in this study, compared to numerous measurements made by *Freyer* [1991] across several years, and changes in the $\delta^{15}\text{N}$ of rain of up to 8.8‰ have been observed over the course of single precipitation events [*Buda and DeWalle*, 2009].

Changes in $\delta^{18}\text{O}$ due to transport are less understood but if affected similarly to $\delta^{15}\text{N}$, the linear $\delta^{18}\text{O}$ versus $\delta^{15}\text{N}$ relationships in Sections II and III could, hypothetically, be attributed to transport effects assuming that the initial isotopic composition is that of dry season nitrate (i.e., $\delta^{15}\text{N} \approx 0\text{‰}$, $\delta^{18}\text{O} \approx 55\text{‰}$). Buda and DeWalle [2009], however, found no correspondence between $\delta^{18}\text{O}$ and $\delta^{15}\text{N}$ in nitrate collected during and between precipitation events.

Mass-dependent fractionation during transport would not influence $\Delta^{17}\text{O}$, but both $\delta^{18}\text{O}$ and $\Delta^{17}\text{O}$ have been shown to vary between different sizes of aerosol nitrate, with higher values in coarser particles [Patris *et al.*, 2007; Morin *et al.*, 2009]. These results were attributed to nitrate formation by different oxidation pathways. Morin *et al.* [2009] found no difference in $\delta^{15}\text{N}$ between size fractions collected over the southeastern tropical Atlantic, suggesting that $\delta^{15}\text{N}$ was not affected by aerosol formation, and concluded that $\delta^{15}\text{N}$ in the remote low latitudes may thus reflect NO_x sources.

The $\delta^{15}\text{N}$ signatures of NO_x sources have been constrained to varying degrees and represent a critical subject of ongoing research. Lightning NO_x is thought to be close to 0‰ based on laboratory experiments [Hoering, 1957]. NO_x produced by microbial processes in fertilized soils was found to be strongly negative (−48.9 to −19.9‰) [Li and Wang, 2008], in accord with predictions [Freyer, 1978]. NO_x formed by the oxidation of N_2O in the stratosphere has been estimated to be close to 19‰ [Savarino *et al.*, 2007]. The $\delta^{15}\text{N}$ of NO_x produced by fossil fuel combustion has been observed and suggested to be both positive and negative [see Hastings *et al.*, 2009; Felix *et al.*, 2012, and references therein]. No direct measurements exist for biomass burning despite the recognized importance of this source. As with fossil fuel combustion, the $\delta^{15}\text{N}$ of the produced NO_x is likely to vary with temperature and the composition of the initial material. The high $\delta^{15}\text{N}$ of nitrate in preindustrial ice from Greenland may indicate a positive composition [Hastings *et al.*, 2005, 2009], but negative values have also been indirectly suggested based on laboratory burning experiments [Turekian *et al.*, 1998].

With regard to the contribution of nitrate sources to the QIC, fossil fuel combustion is likely negligible given the remote and sparsely populated air mass source regions [Levy *et al.*, 1999; Jaeglé *et al.*, 2005]. The dry season $\delta^{15}\text{N}$ of ~0‰ in Sections II and III compares well with that expected from lightning, which is estimated to be the dominant source of NO_x in the tropical midtroposphere and upper troposphere [Levy *et al.*, 1996, 1999]. The higher-altitude nature of this source would also be consistent with the higher $\delta^{18}\text{O}$ and $\Delta^{17}\text{O}$ compositions reflecting increases in NO_x cycling by O_3 and nitrate formation via N_2O_5 hydrolysis (section 5.6.1). Nitrate salts in the Atacama Desert of Chile, which have $\delta^{15}\text{N}$ (and $\delta^{18}\text{O}$) compositions similar to that of QND30 dry season nitrate, have also been attributed to lightning [Michalski *et al.*, 2004a], but transport of these salts to the QIC is not consistent with the prevailing regional winds and influence of topography (Figure 1 and section 2). Given our current understanding of microbially produced NO_x , the lower $\delta^{15}\text{N}$ observed during wet seasons may reflect a biogenic source in the Amazon Basin. Based on modeling, such emissions are suggested to represent the largest contribution to NO_x in the lower troposphere over the region during this time of the year [Levy *et al.*, 1999].

6. Conclusions

A low-latitude, high-elevation ice core from the Quelccaya Ice Cap in southeastern Peru provides the first record of the isotopic composition of atmospheric nitrate as preserved in tropical ice. This marks an initial step in developing tropical ice cores as continuous and long-term archives of nitrate- $\delta^{15}\text{N}$, $-\delta^{18}\text{O}$, and $-\Delta^{17}\text{O}$ for a region of the planet where no other such histories are currently available. Given the susceptibility of nitrate to postdepositional loss and isotopic fractionation, we have assessed the influence of photolysis and HNO_3 evaporation and, based on our current understanding of these processes, find no evidence for such alteration below ~12 m depth. This preservation may have been promoted by a high snow accumulation rate, alkalinity in the snow, and the effect of high impurity concentrations on light penetration. The nitrate profiles of the upper ~12 m and a snowpit from 2011, however, may reflect alteration facilitated by recent melting at the surface. Limited intervals marked by very low $[\text{NO}_3^-]$ near the bottom (~30 m) of the core may have also been affected by meltwater. In the unaltered sections, clear seasonal cycles in isotopic composition and $[\text{NO}_3^-]$ exist, with dry seasons marked by high $\delta^{15}\text{N}$, $\delta^{18}\text{O}$, $\Delta^{17}\text{O}$, and $[\text{NO}_3^-]$, while low values are observed during wet seasons. Rainout effects during transport and in situ production by nitrification cannot be ruled

out at this time, but our results are consistent with mixing of atmospheric nitrate derived from discrete and seasonally dependent NO_x sources and oxidation pathways. Future work should include concurrent atmospheric, surface snow, and snowpit sampling, but our findings suggest that higher, colder, and dustier low-latitude glaciers in the Andes and Himalayas would likely be suitable for future isotopic studies of nitrate in ice.

Acknowledgments

The authors wish to thank Mary Davis for her assistance throughout this project, Doug Hardy for helpful meteorological data and discussion, and two anonymous reviewers for their thoughtful comments. Field assistance and support were provided by Félix Benjamin Vicencio and Vicencio Expeditions, the Explorers Club Exploration Fund, the American Philosophical Society Lewis and Clark Award, and the Brown University Graduate School. This is Byrd Polar Research Center contribution C-1435.

References

- Abida, O., and H. D. Osthoff (2011), On the pH dependence of photo-induced volatilization of nitrogen oxides from frozen solutions containing nitrate, *Geophys. Res. Lett.*, *38*, L16808, doi:10.1029/2011GL048517.
- Alexander, B., J. Savarino, K. J. Kreutz, and M. H. Thiemens (2004), Impact of preindustrial biomass-burning emissions on the oxidation pathways of tropospheric sulfur and nitrogen, *J. Geophys. Res.*, *109*, D08303, doi:10.1029/2003JD004218.
- Alexander, B., M. G. Hastings, D. J. Allman, J. Dachs, J. A. Thornton, and S. A. Kunasek (2009), Quantifying atmospheric nitrate formation pathways based on a global model of the oxygen isotopic composition ($\Delta^{17}\text{O}$) of atmospheric nitrate, *Atmos. Chem. Phys.*, *9*(14), 5043–5056, doi:10.5194/acp-9-5043-2009.
- Amoroso, A., H. J. Beine, R. Sparapani, M. Nardino, and I. Allegrini (2006), Observation of coinciding arctic boundary layer ozone depletion and snow surface emissions of nitrous acid, *Atmos. Environ.*, *40*(11), 1949–1956, doi:10.1016/j.atmosenv.2005.11.027.
- Amoroso, A., et al. (2010), Microorganisms in dry polar snow are involved in the exchanges of reactive nitrogen species with the atmosphere, *Environ. Sci. Technol.*, *44*(2), 714–719, doi:10.1021/es9027309.
- Andreae, M. O., et al. (1988), Biomass-burning emissions and associated haze layers over Amazonia, *J. Geophys. Res.*, *93*(D2), 1509–1527, doi:10.1029/JD093id02p01509.
- Anenberg, S. C., et al. (2009), Intercontinental impacts of ozone pollution on human mortality, *Environ. Sci. Technol.*, *43*(17), 6482–6487, doi:10.1021/es900518z.
- Baker, A. R., K. Weston, S. D. Kelly, M. Voss, P. Streu, and J. N. Cape (2007), Dry and wet deposition of nutrients from the tropical Atlantic atmosphere: Links to primary productivity and nitrogen fixation, *Deep Sea Res., Part I*, *54*(10), 1704–1720, doi:10.1016/j.dsr.2007.07.001.
- Barkan, E., and B. Luz (2005), High precision measurements of $^{17}\text{O}/^{16}\text{O}$ and $^{18}\text{O}/^{16}\text{O}$ ratios in H_2O , *Rapid Commun. Mass Spectrom.*, *19*(24), 3737–3742, doi:10.1002/rcm.2250.
- Begun, G. M., and C. E. Melton (1956), Nitrogen isotopic fractionation between NO and NO_2 and mass discrimination in mass analysis of NO_2 , *J. Chem. Phys.*, *25*(6), 1292–1293, doi:10.1063/1.1743215.
- Beine, H. J., F. Dominé, W. Simpson, R. E. Honrath, R. Sparapani, X. Zhou, and M. King (2002), Snow-pile and chamber experiments during the Polar Sunrise Experiment 'Alert 2000': Exploration of nitrogen chemistry, *Atmos. Environ.*, *36*(15–16), 2707–2719, doi:10.1016/s1352-2310(02)00120-6.
- Beine, H. J., F. Dominé, A. Ianniello, M. Nardino, I. Allegrini, K. Teinilä, and R. Hillamo (2003), Fluxes of nitrates between snow surfaces and the atmosphere in the European high Arctic, *Atmos. Chem. Phys.*, *3*(2), 335–346, doi:10.5194/acp-3-335-2003.
- Beine, H. J., A. Amoroso, F. Dominé, M. D. King, M. Nardino, A. Ianniello, and J. L. France (2006), Surprisingly small HONO emissions from snow surfaces at Browning Pass, Antarctica, *Atmos. Chem. Phys.*, *6*(9), 2569–2580, doi:10.5194/acp-6-2569-2006.
- Blunier, T., G. L. Floch, H.-W. Jacobi, and E. Quansah (2005), Isotopic view on nitrate loss in Antarctic surface snow, *Geophys. Res. Lett.*, *32*, L13501, doi:10.1029/2005GL023011.
- Böhlke, J. K., S. J. Mroczkowski, and T. B. Coplen (2003), Oxygen isotopes in nitrate: New reference materials for $^{18}\text{O}/^{16}\text{O}$ measurements and observations on nitrate-water equilibration, *Rapid Commun. Mass Spectrom.*, *17*(16), 1835–1846, doi:10.1002/rcm.1123.
- Bradley, R. S., F. T. Keimig, H. F. Diaz, and D. R. Hardy (2009), Recent changes in freezing level heights in the tropics with implications for the deglaciation of high mountain regions, *Geophys. Res. Lett.*, *36*, L17701, doi:10.1029/2009GL037712.
- Brothers, L. A., G. Dominguez, P. Fabian, and M. H. Thiemens (2008), Using multi-isotope tracer methods to understand the sources of nitrate in aerosols, fog and river water in Podocarpus National Forest, Ecuador, *Eos Trans. AGU*, *89*(53), Fall Meet. Suppl., Abstract A11C-0136.
- Buda, A. R., and D. R. DeWalle (2009), Using atmospheric chemistry and storm track information to explain the variation of nitrate stable isotopes in precipitation at a site in central Pennsylvania, USA, *Atmos. Environ.*, *43*(29), 4453–4464, doi:10.1016/j.atmosenv.2009.06.027.
- Buffen, A. M., L. G. Thompson, E. Mosley-Thompson, and K. I. Huh (2009), Recently exposed vegetation reveals Holocene changes in the extent of the Quelccaya Ice Cap, Peru, *Quat. Res.*, *72*(2), 157–163, doi:10.1016/j.yqres.2009.02.007.
- Bunton, C. A., E. A. Halevi, and D. R. Llewellyn (1952), Oxygen exchange between nitric acid and water. Part I, *J. Chem. Soc.*, 4913–4916, doi:10.1039/jr9520004913.
- Burkhart, J. F., M. Hutterli, R. C. Bales, and J. R. McConnell (2004), Seasonal accumulation timing and preservation of nitrate in firn at Summit, Greenland, *J. Geophys. Res.*, *109*, D19302, doi:10.1029/2004JD004658.
- Burkhart, J. F., R. C. Bales, J. R. McConnell, and M. A. Hutterli (2006), Influence of North Atlantic Oscillation on anthropogenic transport recorded in northwest Greenland ice cores, *J. Geophys. Res.*, *111*, D22309, doi:10.1029/2005JD006771.
- Burkhart, J. F., R. C. Bales, J. R. McConnell, M. A. Hutterli, and M. M. Frey (2009), Geographic variability of nitrate deposition and preservation over the Greenland Ice Sheet, *J. Geophys. Res.*, *114*, D06301, doi:10.1029/2008JD010600.
- Campen, R. K., T. Sowers, and R. B. Alley (2003), Evidence of microbial consortia metabolizing within a low-latitude mountain glacier, *Geology*, *31*(3), 231–234, doi:10.1130/0091-7613(2003)031<0231:eomcmw>2.0.co;2.
- Casciotti, K. L., D. M. Sigman, M. G. Hastings, J. K. Böhlke, and A. Hilkert (2002), Measurement of the oxygen isotopic composition of nitrate in seawater and freshwater using the denitrifier method, *Anal. Chem.*, *74*(19), 4905–4912, doi:10.1021/ac020113w.
- Chu, L., and C. Anastasio (2003), Quantum yields of hydroxyl radical and nitrogen dioxide from the photolysis of nitrate on ice, *J. Phys. Chem. A*, *107*(45), 9594–9602, doi:10.1021/jp034913z.
- Cragin, J. H., and R. McGilvary (1995), Can inorganic chemical species volatilize from snow?, in *Biogeochemistry of Seasonally Snow-Covered Catchments*, edited by K. A. Tonnessen, M. W. Williams, and M. Tranter, pp. 11–16, IAHS Press, Wallingford, U. K.
- Criss, R. E. (1999), *Principles of Stable Isotope Distribution*, Oxford Univ. Press, New York.
- Crutzen, P. J., and J. Lelieveld (2001), Human impacts on atmospheric chemistry, *Ann. Rev. Earth Planet. Sci.*, *29*(1), 17–45, doi:10.1146/annurev.earth.29.1.17.
- Davies, T. D., C. E. Vincent, and P. Brimblecombe (1982), Preferential elution of strong acids from a Norwegian ice cap, *Nature*, *300*(5888), 161–163, doi:10.1038/300161a0.

- Delmas, R., D. Serça, and C. Jambert (1997), Global inventory of NO_x sources, *Nutr. Cycling Agroecosyst.*, *48*(1), 51–60, doi:10.1023/a:1009793806086.
- Dibb, J. E., and M. Fahnstocck (2004), Snow accumulation, surface height change, and firn densification at Summit, Greenland: Insights from 2 years of in situ observation, *J. Geophys. Res.*, *109*, D24113, doi:10.1029/2003JD004300.
- Dibb, J. E., R. W. Talbot, J. W. Munger, D. J. Jacob, and S.-M. Fan (1998), Air-snow exchange of HNO₃ and NO_y at Summit, Greenland, *J. Geophys. Res.*, *103*(D3), 3475–3486, doi:10.1029/97JD03132.
- Dibb, J. E., M. Arsenaault, M. C. Peterson, and R. E. Honrath (2002), Fast nitrogen oxide photochemistry in Summit, Greenland snow, *Atmos. Environ.*, *36*(15–16), 2501–2511, doi:10.1016/s1352-2310(02)00130-9.
- Dibb, J. E., S. I. Whitlow, and M. Arsenaault (2007), Seasonal variations in the soluble ion content of snow at Summit, Greenland: Constraints from three years of daily surface snow samples, *Atmos. Environ.*, *41*(24), 5007–5019, doi:10.1016/j.atmosenv.2006.12.010.
- Dubey, M. K., R. Mohrschladt, N. M. Donahue, and J. G. Anderson (1997), Isotope specific kinetics of hydroxyl radical (OH) with water (H₂O): Testing models of reactivity and atmospheric fractionation, *J. Phys. Chem. A*, *101*(8), 1494–1500, doi:10.1021/jp962332p.
- Dubowski, Y., A. J. Colussi, and M. R. Hoffmann (2001), Nitrogen dioxide release in the 302 nm band photolysis of spray-frozen aqueous nitrate solutions: Atmospheric implications, *J. Phys. Chem. A*, *105*(20), 4928–4932, doi:10.1021/jp0042009.
- Dubowski, Y., A. J. Colussi, C. Boxe, and M. R. Hoffmann (2002), Monotonic increase of nitrite yields in the photolysis of nitrate in ice and water between 238 and 294 K, *J. Phys. Chem. A*, *106*(30), 6967–6971, doi:10.1021/jp0142942.
- Eichler, A., M. Schwikowski, and H. W. Gäggeler (2001), Meltwater-induced relocation of chemical species in Alpine firn, *Tellus B*, *53*(2), 192–203, doi:10.1034/j.1600-0889.2001.d01-15.x.
- Elliott, E. M., C. Kendall, S. D. Wankel, D. A. Burns, E. W. Boyer, K. Harlin, D. J. Bain, and T. J. Butler (2007), Nitrogen isotopes as indicators of NO_x source contributions to atmospheric nitrate deposition across the midwestern and northeastern United States, *Environ. Sci. Technol.*, *41*(22), 7661–7667, doi:10.1021/es070898t.
- Elliott, E. M., C. Kendall, E. W. Boyer, D. A. Burns, G. G. Lear, H. E. Golden, K. Harlin, A. Bytnerowicz, T. J. Butler, and R. Glatz (2009), Dual nitrate isotopes in dry deposition: Utility for partitioning NO_x source contributions to landscape nitrogen deposition, *J. Geophys. Res.*, *114*, G04020, doi:10.1029/2008JG000889.
- Elsler, J. J., T. Andersen, J. S. Baron, A.-K. Bergström, M. Jansson, M. Kyle, K. R. Nydick, L. Steger, and D. O. Hessen (2009), Shifts in lake N:P stoichiometry and nutrient limitation driven by atmospheric nitrogen deposition, *Science*, *326*(5954), 835–837, doi:10.1126/science.1176199.
- Erbland, J., W. C. Vicars, J. Savarino, S. Morin, M. M. Frey, D. Frosini, E. Vince, and J. M. F. Martins (2013), Air-snow transfer of nitrate on the East Antarctic Plateau—Part 1: Isotopic evidence for a photolytically driven dynamic equilibrium in summer, *Atmos. Chem. Phys.*, *13*(13), 6403–6419, doi:10.5194/acp-13-6403-2013.
- Fabian, P., R. Rollenbeck, N. Spichtinger, L. Brothers, G. Dominguez, and M. Thiemens (2009), Sahara dust, ocean spray, volcanoes, biomass burning: Pathways of nutrients into Andean rainforests, *Adv. Geosci.*, *2*, 85–94, doi:10.5194/adgeo-22-85-2009.
- Felix, J. D., E. M. Elliott, and S. L. Shaw (2012), Nitrogen isotopic composition of coal-fired power plant NO_x: Influence of emission controls and implications for global emission inventories, *Environ. Sci. Technol.*, *46*(6), 3528–3535, doi:10.1021/es203355v.
- France, J. L., M. D. King, M. M. Frey, J. Erbland, G. Picard, S. Preunkert, A. MacArthur, and J. Savarino (2011), Snow optical properties at Dome C (Concordia), Antarctica; implications for snow emissions and snow chemistry of reactive nitrogen, *Atmos. Chem. Phys.*, *11*(18), 9787–9801, doi:10.5194/acp-11-9787-2011.
- Frey, M. M., J. Savarino, S. Morin, J. Erbland, and J. M. F. Martins (2009), Photolysis imprint in the nitrate stable isotope signal in snow and atmosphere of East Antarctica and implications for reactive nitrogen cycling, *Atmos. Chem. Phys.*, *9*(22), 8681–8696, doi:10.5194/acp-9-8681-2009.
- Freyer, H. D. (1978), Preliminary ¹⁵N studies on atmospheric nitrogenous trace gases, *Pure Appl. Geophys.*, *116*(2), 393–404, doi:10.1007/bf01636894.
- Freyer, H. D. (1991), Seasonal variation of ¹⁵N/¹⁴N ratios in atmospheric nitrate species, *Tellus B*, *43*(1), 30–44, doi:10.1034/j.1600-0889.1991.00003.x.
- Freyer, H. D., D. Kley, A. Volz-Thomas, and K. Kobel (1993), On the interaction of isotopic exchange processes with photochemical reactions in atmospheric oxides of nitrogen, *J. Geophys. Res.*, *98*(D8), 14,791–14,796, doi:10.1029/93JD00874.
- Freyer, H. D., K. Kobel, R. J. Delmas, D. Kley, and M. R. Legrand (1996), First results of ¹⁵N/¹⁴N ratios in nitrate from alpine and polar ice cores, *Tellus B*, *48*(1), 93–105, doi:10.1034/j.1600-0889.1996.00009.x.
- Galloway, J. N., et al. (2004), Nitrogen cycles: Past, present, and future, *Biogeochemistry*, *70*(2), 153–226, doi:10.1007/s10533-004-0370-0.
- Gao, Y. Q., and R. A. Marcus (2001), Strange and unconventional isotope effects in ozone formation, *Science*, *293*(5528), 259–263, doi:10.1126/science.1058528.
- Garreaud, R., M. Vuille, and A. C. Clement (2003), The climate of the Altiplano: Observed current conditions and mechanisms of past changes, *Palaeogeogr. Palaeoclimatol. Palaeoecol.*, *194*, 5–22, doi:10.1016/s0031-0182(03)00269-4.
- Ginot, P., C. Kull, M. Schwikowski, U. Schotterer, and H. W. Gäggeler (2001), Effects of postdepositional processes on snow composition of a subtropical glacier (Cerro Tapado, Chilean Andes), *J. Geophys. Res.*, *106*(D23), 32,375–32,386, doi:10.1029/2000JD000071.
- Ginot, P., U. Schotterer, W. Stichler, M. A. Godoi, B. Francou, and M. Schwikowski (2010), Influence of the Tungurahua eruption on the ice core records of Chimborazo, Ecuador, *Cryosphere*, *4*(4), 561–568, doi:10.5194/tc-4-561-2010.
- Grannas, A. M., et al. (2007), An overview of snow photochemistry: Evidence, mechanisms and impacts, *Atmos. Chem. Phys.*, *7*(16), 4329–4373, doi:10.5194/acp-7-4329-2007.
- Gross, G. W., and R. K. Svec (1997), Effect of ammonium on anion uptake and dielectric relaxation in laboratory-grown ice columns, *J. Phys. Chem. B*, *101*(32), 6282–6284, doi:10.1021/jp963213c.
- Hastings, M. G., D. M. Sigman, and F. Lipschultz (2003), Isotopic evidence for source changes of nitrate in rain at Bermuda, *J. Geophys. Res.*, *108*(D24), 4790, doi:10.1029/2003JD003789.
- Hastings, M. G., E. J. Steig, and D. M. Sigman (2004), Seasonal variations in N and O isotopes of nitrate in snow at Summit, Greenland: Implications for the study of nitrate in snow and ice cores, *J. Geophys. Res.*, *109*, D20306, doi:10.1029/2004JD004991.
- Hastings, M. G., D. M. Sigman, and E. J. Steig (2005), Glacial/interglacial changes in the isotopes of nitrate from the Greenland Ice Sheet Project 2 (GISP2) ice core, *Global Biogeochem. Cycles*, *19*, GB4024, doi:10.1029/2005GB002502.
- Hastings, M. G., J. C. Jarvis, and E. J. Steig (2009), Anthropogenic impacts on nitrogen isotopes of ice-core nitrate, *Science*, *324*(5932), 1288, doi:10.1126/science.1170510.
- Heaton, T. H. E. (1986), Isotopic studies of nitrogen pollution in the hydrosphere and atmosphere: A review, *Chem. Geol.*, *59*(0), 87–102, doi:10.1016/0168-9622(86)90059-x.
- Hoering, T. (1957), The isotopic composition of the ammonia and the nitrate ion in rain, *Geochim. Cosmochim. Acta*, *12*(1–2), 97–102, doi:10.1016/0016-7037(57)90021-2.

- Holtgrieve, G. W., et al. (2011), A coherent signature of anthropogenic nitrogen deposition to remote watersheds of the Northern Hemisphere, *Science*, 334(6062), 1545–1548, doi:10.1126/science.1212267.
- Honrath, R. E., M. C. Peterson, S. Guo, J. E. Dibb, P. B. Shepson, and B. Campbell (1999), Evidence of NO_x production within or upon ice particles in the Greenland snowpack, *Geophys. Res. Lett.*, 26(6), 695–698, doi:10.1029/1999GL900077.
- Honrath, R. E., S. Guo, M. C. Peterson, M. P. Dziobak, J. E. Dibb, and M. A. Arsenault (2000), Photochemical production of gas phase NO_x from ice crystal NO₃, *J. Geophys. Res.*, 105(D19), 24,183–24,190, doi:10.1029/2000JD900361.
- Jacobi, H.-W., and B. Hilker (2007), A mechanism for the photochemical transformation of nitrate in snow, *J. Photochem. Photobiol., A*, 185(2-3), 371–382, doi:10.1016/j.jphotochem.2006.06.039.
- Jaeglé, L., L. Steinberger, R. V. Martin, and K. Chance (2005), Global partitioning of NO_x sources using satellite observations: Relative roles of fossil fuel combustion, biomass burning and soil emissions, *Faraday Discuss.*, 130, 407–423, doi:10.1039/b502128f.
- Janssens, I. A., et al. (2010), Reduction of forest soil respiration in response to nitrogen deposition, *Nat. Geosci.*, 3(5), 315–322, doi:10.1038/ngeo844.
- Jarvis, J. C., E. J. Steig, M. G. Hastings, and S. A. Kunasek (2008), Influence of local photochemistry on isotopes of nitrate in Greenland snow, *Geophys. Res. Lett.*, 35, L21804, doi:10.1029/2008GL035551.
- Jarvis, J. C., M. G. Hastings, E. J. Steig, and S. A. Kunasek (2009), Isotopic ratios in gas-phase HNO₃ and snow nitrate at Summit, Greenland, *J. Geophys. Res.*, 114, D17301, doi:10.1029/2009JD012134.
- Jones, A. E., R. Weller, E. W. Wolff, and H.-W. Jacobi (2000), Speciation and rate of photochemical NO and NO₂ production in Antarctic snow, *Geophys. Res. Lett.*, 27(3), 345–348, doi:10.1029/1999GL010885.
- Kaiser, J., M. G. Hastings, B. Z. Houlton, T. Rockmann, and D. M. Sigman (2007), Triple oxygen isotope analysis of nitrate using the denitrifier method and thermal decomposition of N₂O, *Anal. Chem.*, 79(2), 599–607, doi:10.1021/ac061022s.
- Kanamitsu, M., W. Ebisuzaki, J. Woollen, S.-K. Yang, J. J. Hnilo, M. Fiorino, and G. L. Potter (2002), NCEP-DOE AMIP-II Reanalysis (R-2), *Bull. Am. Meteorol. Soc.*, 83(11), 1631–1643, doi:10.1175/bams-83-11-1631.
- Kehrwald, N. M., C. I. Czimczik, G. M. Santos, L. G. Thompson, and L. Ziolkowski (2008), Concentration and ¹⁴C content of total organic carbon and black carbon in small (<100 μg C) samples from low-latitude alpine ice cores, *Eos Trans. AGU*, 89(53), Fall Meet. Suppl., Abstract C41C-0536.
- Kendall, C., E. M. Elliott, and S. D. Wankel (2007), Tracing anthropogenic inputs of nitrogen to ecosystems, in *Stable Isotopes in Ecology and Environmental Science*, edited by K. Lajtha and R. H. Michener, pp. 375–449, Blackwell, Oxford, U. K., doi:10.1002/9780470691854.ch12.
- Kunasek, S. A., B. Alexander, E. J. Steig, M. G. Hastings, D. J. Gleason, and J. C. Jarvis (2008), Measurements and modeling of Δ¹⁷O of nitrate in snowpits from Summit, Greenland, *J. Geophys. Res.*, 113, D24302, doi:10.1029/2008JD010103.
- Lee, D. S., I. Köhler, E. Grobler, F. Rohrer, R. Sausen, L. Gallardo-Klenner, J. G. J. Olivier, F. J. Dentener, and A. F. Bouwman (1997), Estimations of global NO_x emissions and their uncertainties, *Atmos. Environ.*, 31(12), 1735–1749, doi:10.1016/s1352-2310(96)00327-5.
- Legrand, M., E. Wolff, and D. Wagenbach (1999), Antarctic aerosol and snowfall chemistry: Implications for deep Antarctic ice-core chemistry, *Ann. Glaciol.*, 29, 66–72, doi:10.3189/172756499781821094.
- Lehmann, M. F., P. Reichert, S. M. Bernasconi, A. Barbieri, and J. A. McKenzie (2003), Modelling nitrogen and oxygen isotope fractionation during denitrification in a lacustrine redox-transition zone, *Geochim. Cosmochim. Acta*, 67(14), 2529–2542, doi:10.1016/s0016-7037(03)00085-1.
- Levy, H., II, W. J. Moxim, and R. S. Kasibhatla (1996), A global three-dimensional time-dependent lightning source of tropospheric NO_x, *J. Geophys. Res.*, 101(D17), 22,911–22,922, doi:10.1029/96JD02341.
- Levy, H., II, W. J. Moxim, A. A. Klonecki, and P. S. Kasibhatla (1999), Simulated tropospheric NO_x: Its evaluation, global distribution and individual source contributions, *J. Geophys. Res.*, 104(D21), 26,279–26,306, doi:10.1029/1999JD900442.
- Li, D., and X. Wang (2008), Nitrogen isotopic signature of soil-released nitric oxide (NO) after fertilizer application, *Atmos. Environ.*, 42(19), 4747–4754, doi:10.1016/j.atmosenv.2008.01.042.
- Likens, G. E., and F. H. Bormann (1974), Acid rain: A serious regional environmental problem, *Science*, 184(4142), 1176–1179, doi:10.1126/science.184.4142.1176.
- Madronich, S., and S. Flocke (1998), The role of solar radiation in atmospheric chemistry, in *Handbook of Environmental Chemistry*, edited by P. Boule, pp. 1–26, Springer-Verlag, Berlin, Germany.
- Mariotti, A., A. Landreau, and B. Simon (1988), ¹⁵N isotope biogeochemistry and natural denitrification process in groundwater: Application to the chalk aquifer of northern France, *Geochim. Cosmochim. Acta*, 52(7), 1869–1878, doi:10.1016/0016-7037(88)90010-5.
- Mayewski, P. A., and M. R. Legrand (1990), Recent increase in nitrate concentration of Antarctic snow, *Nature*, 346(6281), 258–260, doi:10.1038/346258a0.
- Mayewski, P. A., W. B. Lyons, M. J. Spencer, M. S. Twickler, C. F. Buck, and S. Whitlow (1990), An ice-core record of atmospheric response to anthropogenic sulphate and nitrate, *Nature*, 346(6284), 554–556, doi:10.1038/346554a0.
- McCabe, J. R., C. S. Boxe, A. J. Colussi, M. R. Hoffmann, and M. H. Thiemens (2005), Oxygen isotopic fractionation in the photochemistry of nitrate in water and ice, *J. Geophys. Res.*, 110, D15310, doi:10.1029/2004JD005484.
- Meijer, H. A. J., and W. J. Li (1998), The use of electrolysis for accurate δ¹⁷O and δ¹⁸O isotope measurements in water, *Isot. Environ. Health Stud.*, 34(4), 349–369, doi:10.1080/10256019808234072.
- Michalski, G., J. Savariño, J. K. Böhlke, and M. Thiemens (2002), Determination of the total oxygen isotopic composition of nitrate and the calibration of a Δ¹⁷O nitrate reference material, *Anal. Chem.*, 74(19), 4989–4993, doi:10.1021/ac0256282.
- Michalski, G., Z. Scott, M. Kabling, and M. H. Thiemens (2003), First measurements and modeling of Δ¹⁷O in atmospheric nitrate, *Geophys. Res. Lett.*, 30, 1870, doi:10.1029/2003GL017015.
- Michalski, G., J. K. Böhlke, and M. Thiemens (2004a), Long term atmospheric deposition as the source of nitrate and other salts in the Atacama Desert, Chile: New evidence from mass-independent oxygen isotopic compositions, *Geochim. Cosmochim. Acta*, 68(20), 4023–4038, doi:10.1016/j.gca.2004.04.009.
- Michalski, G., T. Meixner, M. Fenn, L. Hernandez, A. Sirulnik, E. Allen, and M. Thiemens (2004b), Tracing atmospheric nitrate deposition in a complex semiarid ecosystem using Δ¹⁷O, *Environ. Sci. Technol.*, 38(7), 2175–2181, doi:10.1021/es034980+.
- Michalski, G., J. G. Bockheim, C. Kendall, and M. Thiemens (2005), Isotopic composition of Antarctic Dry Valley nitrate: Implications for NO_x sources and cycling in Antarctica, *Geophys. Res. Lett.*, 32, L13817, doi:10.1029/2004GL022121.
- Michalski, G., S. K. Bhattacharya, and D. F. Mase (2011), Oxygen isotope dynamics of atmospheric nitrate and its precursor molecules, in *Handbook of Environmental Isotope Geochemistry*, edited by M. Baskaran, pp. 613–635, Springer-Verlag, Berlin, Germany, doi:10.1007/978-3-642-10637-8_30.
- Miller, M. F. (2002), Isotopic fractionation and the quantification of ¹⁷O anomalies in the oxygen three-isotope system: An appraisal and geochemical significance, *Geochim. Cosmochim. Acta*, 66(11), 1881–1889, doi:10.1016/s0016-7037(02)00832-3.

- Miller, C. E., and Y. L. Yung (2000), Photo-induced isotopic fractionation, *J. Geophys. Res.*, *105*(D23), 29,039–29,051, doi:10.1029/2000JD900388.
- Miteva, V., T. Sowers, and J. Brenchley (2007), Production of N₂O by ammonia oxidizing bacteria at subfreezing temperatures as a model for assessing the N₂O anomalies in the Vostok ice core, *Geomicrobiol. J.*, *24*(5), 451–459, doi:10.1080/01490450701437693.
- Morin, S., J. Savarino, S. Bekki, A. Cavender, P. B. Shepson, and J. W. Bottenheim (2007a), Major influence of BrO on the NO_x and nitrate budgets in the Arctic spring, inferred from Δ¹⁷O(NO₃⁻) measurements during ozone depletion events, *Environ. Chem.*, *4*(4), 238–241, doi:10.1071/en07003.
- Morin, S., J. Savarino, S. Bekki, S. Gong, and J. W. Bottenheim (2007b), Signature of Arctic surface ozone depletion events in the isotope anomaly (Δ¹⁷O) of atmospheric nitrate, *Atmos. Chem. Phys.*, *7*, 1451–1469, doi:10.5194/acp-7-1451-2007.
- Morin, S., J. Savarino, M. M. Frey, N. Yan, S. Bekki, J. W. Bottenheim, and J. M. F. Martins (2008), Tracing the origin and fate of NO_x in the arctic atmosphere using stable isotopes in nitrate, *Science*, *322*(5902), 730–732, doi:10.1126/science.1161910.
- Morin, S., J. Savarino, M. M. Frey, F. Dominé, H.-W. Jacobi, L. Kaleschke, and J. M. F. Martins (2009), Comprehensive isotopic composition of atmospheric nitrate in the Atlantic Ocean boundary layer from 65°S to 79°N, *J. Geophys. Res.*, *114*, D05303, doi:10.1029/2008JD010696.
- Morin, S., R. Sander, and J. Savarino (2011), Simulation of the diurnal variations of the oxygen isotope anomaly (Δ¹⁷O) of reactive atmospheric species, *Atmos. Chem. Phys.*, *11*(8), 3653–3671, doi:10.5194/acp-11-3653-2011.
- Morin, S., J. Erbland, J. Savarino, F. Domine, J. Bock, U. Friess, H.-W. Jacobi, H. Sihler, and J. M. F. Martins (2012), An isotopic view on the connection between photolytic emissions of NO_x from the Arctic snowpack and its oxidation by reactive halogens, *J. Geophys. Res.*, *117*, D00R08, doi:10.1029/2011JD016618.
- Mulvaney, R., and E. W. Wolff (1993), Evidence for winter/spring denitrification of the stratosphere in the nitrate record of Antarctic firn cores, *J. Geophys. Res.*, *98*(D3), 5213–5220, doi:10.1029/92JD02966.
- Mulvaney, R., D. Wagenbach, and E. W. Wolff (1998), Postdepositional change in snowpack nitrate from observation of year-round near-surface snow in coastal Antarctica, *J. Geophys. Res.*, *103*(D9), 11,021–11,031, doi:10.1029/97JD03624.
- Naftz, D. L., P. F. Schuster, and C. A. Johnson (2011), A 50-year record of NO_x and SO₂ sources in precipitation in the Northern Rocky Mountains, USA, *Geochem. Trans.*, *12*(1), 1–10, doi:10.1186/1467-4866-12-4.
- Patris, N., S. S. Cliff, P. K. Quinn, M. Kasem, and M. H. Thiemens (2007), Isotopic analysis of aerosol sulfate and nitrate during ITCT-2 k2: Determination of different formation pathways as a function of particle size, *J. Geophys. Res.*, *112*, D23301, doi:10.1029/2005JD006214.
- Pichlmayer, F., W. Schöner, P. Seibert, W. Stichter, and D. Wagenbach (1998), Stable isotope analysis for characterization of pollutants at high elevation alpine sites, *Atmos. Environ.*, *32*(23), 4075–4085, doi:10.1016/s1352-2310(97)00405-6.
- Potter, C., V. Brooks-Genovese, S. Klooster, and A. Torregrosa (2002), Biomass burning emissions of reactive gases estimated from satellite data analysis and ecosystem modeling for the Brazilian Amazon region, *J. Geophys. Res.*, *107*(D20), 8056, doi:10.1029/2000JD000250.
- Reese, C. A., and K.-B. Liu (2002), Pollen dispersal and deposition on the Quelccaya Ice Cap, Peru, *Phys. Geogr.*, *23*(1), 44–58, doi:10.2747/0272-3646.23.1.44.
- Röthlisberger, R., M. A. Hutterli, S. Sommer, E. W. Wolff, and R. Mulvaney (2000), Factors controlling nitrate in ice cores: Evidence from the Dome C deep ice core, *J. Geophys. Res.*, *105*(D16), 20,565–20,572, doi:10.1029/2000JD900264.
- Röthlisberger, R., et al. (2002), Nitrate in Greenland and Antarctic ice cores: A detailed description of post-depositional processes, *Ann. Glaciol.*, *35*, 209–216, doi:10.3189/172756402781817220.
- Sato, K., N. Takenaka, H. Bandow, and Y. Maeda (2008), Evaporation loss of dissolved volatile substances from ice surfaces, *J. Phys. Chem. A*, *112*(33), 7600–7607, doi:10.1021/jp075551r.
- Savarino, J., and S. Morin (2011), The N, O, S isotopes of oxy-anions in ice cores and polar environments, in *Handbook of Environmental Isotope Geochemistry*, edited by M. Baskaran, pp. 835–864, Springer-Verlag, Berlin, Germany, doi:10.1007/978-3-642-10637-8_39.
- Savarino, J., J. Kaiser, S. Morin, D. M. Sigman, and M. H. Thiemens (2007), Nitrogen and oxygen isotopic constraints on the origin of atmospheric nitrate in coastal Antarctica, *Atmos. Chem. Phys.*, *7*(8), 1925–1945, doi:10.5194/acp-7-1925-2007.
- Savarino, J., S. K. Bhattacharya, S. Morin, M. Baroni, and J. F. Doussin (2008), The NO + O₃ reaction: A triple oxygen isotope perspective on the reaction dynamics and atmospheric implications for the transfer of the ozone isotope anomaly, *J. Chem. Phys.*, *128*(19), 194,303, doi:10.1063/1.2917581.
- Schwarz, M., Y. Oelmann, and W. Wilcke (2011), Stable N isotope composition of nitrate reflects N transformations during the passage of water through a montane rain forest in Ecuador, *Biogeochemistry*, *102*(1-3), 195–208, doi:10.1007/s10533-010-9434-5.
- Schwikowski, M., S. Brütsch, H. W. Gäggeler, and U. Schotterer (1999), A high-resolution air chemistry record from an Alpine ice core: Fiescherhorn glacier, Swiss Alps, *J. Geophys. Res.*, *104*(D11), 13,709–13,719, doi:10.1029/1998JD100112.
- Seinfeld, J. H., and S. N. Pandis (2006), *Atmospheric Chemistry and Physics: From Air Pollution to Climate Change*, John Wiley, Hoboken, N. J.
- Shen, Q. R., W. Ran, and Z. H. Cao (2003), Mechanisms of nitrite accumulation occurring in soil nitrification, *Chemosphere*, *50*(6), 747–753, doi:10.1016/s0045-6535(02)00215-1.
- Shindell, D. T., G. Faluvegi, D. M. Koch, G. A. Schmidt, N. Unger, and S. E. Bauer (2009), Improved attribution of climate forcing to emissions, *Science*, *326*(5953), 716–718, doi:10.1126/science.1174760.
- Sigman, D. M., K. L. Casciotti, M. Andreani, C. Barford, M. Galanter, and J. K. Böhlke (2001), A bacterial method for the nitrogen isotopic analysis of nitrate in seawater and freshwater, *Anal. Chem.*, *73*(17), 4145–4153, doi:10.1021/ac010088e.
- Thibert, E., and F. Dominé (1998), Thermodynamics and kinetics of the solid solution of HNO₃ in ice, *J. Phys. Chem. B*, *102*(22), 4432–4439, doi:10.1021/jp980569a.
- Thiemens, M. H. (1999), Mass-independent isotope effects in planetary atmospheres and the early solar system, *Science*, *283*(5400), 341–345, doi:10.1126/science.283.5400.341.
- Thompson, A. M. (1992), The oxidizing capacity of the Earth's atmosphere: Probable past and future changes, *Science*, *256*(5060), 1157–1165, doi:10.1126/science.256.5060.1157.
- Thompson, L. G., and E. Mosley-Thompson (1982), Spatial distribution of microparticles within Antarctic snow-fall, *Ann. Glaciol.*, *3*, 300–306.
- Thompson, L. G., S. Hastenrath, and B. M. Arno (1979), Climatic ice core records from the tropical Quelccaya Ice Cap, *Science*, *203*(4386), 1240–1243, doi:10.1126/science.203.4386.1240.
- Thompson, L. G., E. Mosley-Thompson, J. F. Bolzan, and B. R. Koci (1985), A 1500-year record of tropical precipitation in ice cores from the Quelccaya Ice Cap, Peru, *Science*, *229*(4717), 971–973, doi:10.1126/science.229.4717.971.
- Thompson, L. G., E. Mosley-Thompson, W. Dansgaard, and P. M. Grootes (1986), The Little Ice Age as recorded in the stratigraphy of the Tropical Quelccaya Ice Cap, *Science*, *234*(4774), 361–364, doi:10.1126/science.234.4774.361.
- Thompson, L. G., E. Mosley-Thompson, M. E. Davis, P.-N. Lin, K. A. Henderson, J. Cole-Dai, J. F. Bolzan, and K.-B. Liu (1995), Late Glacial Stage and Holocene tropical ice core records from Huascarán, Peru, *Science*, *269*(5220), 46–50, doi:10.1126/science.269.5220.46.
- Thompson, L. G., et al. (1998), A 25,000-year tropical climate history from Bolivian ice cores, *Science*, *282*(5395), 1858–1864, doi:10.1126/science.282.5395.1858.

- Thompson, L. G., E. Mosley-Thompson, H. Brecher, M. Davis, B. León, D. Les, P.-N. Lin, T. Mashiotta, and K. Mountain (2006), Abrupt tropical climate change: Past and present, *Proc. Natl. Acad. Sci. U. S. A.*, *103*(28), 10,536–10,543, doi:10.1073/pnas.0603900103.
- Thompson, L. G., H. H. Brecher, E. Mosley-Thompson, D. R. Hardy, and B. G. Mark (2009), Glacier loss on Kilimanjaro continues unabated, *Proc. Natl. Acad. Sci. U. S. A.*, *106*(47), 19,770–19,775, doi:10.1073/pnas.0906029106.
- Thompson, L. G., E. Mosley-Thompson, M. E. Davis, V. S. Zagorodnov, I. M. Howat, V. N. Mikhailenko, and P.-N. Lin (2013), Annually resolved ice core records of tropical climate variability over the past ~1800 years, *Science*, *340*(6135), 945–950, doi:10.1126/science.1234210.
- Turekian, V. C., S. Macko, D. Ballentine, R. J. Swap, and M. Garstang (1998), Causes of bulk carbon and nitrogen isotopic fractionations in the products of vegetation burns: Laboratory studies, *Chem. Geol.*, *152*(1-2), 181–192, doi:10.1016/s0009-2541(98)00105-3.
- van der Werf, G. R., J. T. Randerson, G. J. Collatz, L. Giglio, P. S. Kasibhatla, A. F. Arellano Jr., S. C. Olsen, and E. S. Kasischke (2004), Continental-scale partitioning of fire emissions during the 1997 to 2001 El Niño/La Niña period, *Science*, *303*(5654), 73–76, doi:10.1126/science.1090753.
- Vicars, W. C., S. K. Bhattacharya, J. Erbland, and J. Savarino (2012), Measurement of the ^{17}O -excess ($\Delta^{17}\text{O}$) of tropospheric ozone using a nitrite-coated filter, *Rapid Commun. Mass Spectrom.*, *26*(10), 1219–1231, doi:10.1002/rcm.6218.
- Vuille, M., R. S. Bradley, and F. Keimig (2000), Interannual climate variability in the Central Andes and its relation to tropical Pacific and Atlantic forcing, *J. Geophys. Res.*, *105*(D10), 12,447–12,460, doi:10.1029/2000JD900134.
- Wagnon, P., R. J. Delmas, and M. Legrand (1999), Loss of volatile acid species from upper firn layers at Vostok, Antarctica, *J. Geophys. Res.*, *104*(D3), 3423–3431, doi:10.1029/98JD02855.
- Ward, B. B. (1996), Nitrification and denitrification: Probing the nitrogen cycle in aquatic environments, *Microbiol. Ecol.*, *32*(3), 247–261, doi:10.1007/bf00183061.
- Warneck, P., and C. Wurzinger (1988), Product quantum yields for the 305-nm photodecomposition of nitrate in aqueous solution, *J. Phys. Chem.*, *92*(22), 6278–6283, doi:10.1021/j100333a022.
- Yienger, J. J., and H. Levy II (1995), Empirical model of global soil-biogenic NO_x emissions, *J. Geophys. Res.*, *100*(D6), 11,447–11,464, doi:10.1029/95JD00370.
- Yung, Y. L., and C. E. Miller (1997), Isotopic fractionation of stratospheric nitrous oxide, *Science*, *278*(5344), 1778–1780, doi:10.1126/science.278.5344.1778.
- Zatko, M. C., T. C. Grenfell, B. Alexander, S. J. Doherty, J. L. Thomas, and X. Yang (2013), The influence of snow grain size and impurities on the vertical profiles of actinic flux and associated NO_x emissions on the Antarctic and Greenland ice sheets, *Atmos. Chem. Phys.*, *13*(7), 3547–3567, doi:10.5194/acp-13-3547-2013.